

JAERI - M  
**85-090**

PROGRESS REPORT ON SAFETY  
RESEARCH OF HIGH-LEVEL WASTE  
MANAGEMENT FOR THE PERIOD  
APRIL 1984 TO MARCH 1985

July 1985

(Eds.) Haruto NAKAMURA and Shingo TASHIRO

JAERI-Mレポートは、日本原子力研究所が不定期に公刊している研究報告書です。  
入手の問合わせは、日本原子力研究所技術情報部情報資料課（〒319-11茨城県那珂郡東海村）あて、お申しこしください。なお、このほかに財団法人原子力弘済会資料センター（〒319-11茨城県那珂郡東海村日本原子力研究所内）で複写による実費頒布をおこなっております。

JAERI-M reports are issued irregularly.

Inquiries about availability of the reports should be addressed to Information Division  
Department of Technical Information, Japan Atomic Energy Research Institute, Tokai-mura, Naka-gun, Ibaraki-ken 319-11, Japan.

©Japan Atomic Energy Research Institute, 1985

編集兼発行 日本原子力研究所  
印刷 いばらき印刷株

Progress Report on Safety Research of High-Level Waste  
Management for the Period April 1984 to March 1985

(Eds) Haruto NAKAMURA and Shingo TASHIRO

Department of Environmental Safety Research  
Tokai Research Establishment, JAERI

(Received June 8, 1985)

Researches on high level waste management in fiscal year of 1984  
is reviewed.

Topics are as following;

- 1) Durability tests of vitrified waste form were carried out, especially tests on leaching behavior. Volatilization of cesium in simulated canister was studied to assess the source term at accidental conditions in storage facilities.
- 2) Diffusion of radionuclides in buffer materials and rock was investigated, and durability test of canister materials started in laboratory for irradiation test and in-situ to use real ground water.

Hot experiments were conducted in the Waste Safety Testing Facility (WASTEF) and in-situ experiments were done in granite rock mass near surface.

Keywords: High Level Radioactive Waste, WASTEF, Durability, Vitrified Waste, Leaching, Canister Material, Buffer Material, Progress Report, SYNROC

1984 年 4 月より 1985 年 3 月までの高レベル廃棄物  
処理処分の安全性研究に関する研究報告  
(昭和 58 年 4 月～昭和 59 年 3 月)

日本原子力研究所東海研究所環境安全研究部  
(編) 中村 治人・田代 晋吾

(1985 年 6 月 8 日受理)

高レベル廃棄物処理処分に関する 1984 年度の研究内容をまとめた。

主な点は次の事項である。

- 1) 廃棄物ガラス固化体の耐久性試験を行った、特に浸出挙動について実施した。また、貯蔵施設の事故時におけるリースタームを評価するため、模擬キャニスタ中の Cs の揮発について研究した。
  - 2) 緩衝材及び岩石中の放射性核種の拡散について研究した。また、キャニスタ材の耐久性試験として、室内照射試験及び実地下水を使うための原位置試験を実施した。
- ホット試験は WASTEF で実施し、原位置試験は地表近くの花崗岩岩盤内で実施した。

## Contents

Introduction .....	1
1. Waste forms examination .....	1
1.1 Leaching behavior of simulated high-level waste glass in groundwater .....	2
1.2 Soxhlet leach test of a devitrified simulated high-level waste glass .....	8
1.3 Tensile strength of simulated high-level waste glass .....	14
1.4 Crystalline product on surface of SYNROC after long leaching .....	18
2. Safety evaluation for geologic disposal .....	25
2.1 Diffusion of radionuclides into rock .....	25
2.2 Gamma-ray irradiation effects on near-field phenomena in geologic repositories for radioactive waste ...	28
2.3 Diffusion of ground water into buffer mass of a simulated disposal pit and research on buffer materials suitable for sorption of Tc .....	33
2.4 Progress with field experiments in granite rock mass .....	38
2.5 In-situ corrosion test .....	45
2.6 Accumulation of informations on characteristics of rock mass at deep underground from surveys for designing underground facilities .....	48
2.7 Numerical model of ground water .....	53
3. Safety examination of vitrified waste forms in the hot cells of WASTE-F .....	59
3.1 Production of radioactive vitrified test samples .....	60
3.2 Development of a recycle system of cooling water containing glass slurry .....	65
3.3 Preliminary experiments on contamination of metallic surfaces caused by HLW glass .....	67
3.4 Volatilization of cesium from nuclear waste glass in a canister .....	70
3.5 Characterization of waste form to be returned from over-seareprocessing .....	76
4. Safety study of nuclear facilities of vitrified HLW's stream .....	77

## 目 次

まえがき .....	1
1. 廃棄物固化体の試験 .....	1
1.1 地下水中での模擬高レベル廃棄物ガラスの浸出挙動 .....	2
1.2 失透した模擬高レベル廃棄物ガラスのソックスレー浸出試験 .....	8
1.3 模擬高レベル廃棄物ガラスの引張り強度 .....	14
1.4 浸出後のSYNROC 表面に生じた結晶 .....	18
2. 地層処分の安全性評価 .....	25
2.1 岩石中への放射性核種の拡散 .....	25
2.2 放射性廃棄物の地層処分における周辺環境に対する $\gamma$ 線照射効果 .....	28
2.3 模擬処分孔中の緩衝材中の地下水の拡散とTcの吸着に適した 緩衝材に関する研究 .....	33
2.4 花崗岩岩盤におけるフィールド試験の進捗状況 .....	38
2.5 原位置腐食試験 .....	45
2.6 地下構築物の設計用調査からの深地層における岩盤の特性に 関する情報の収集 .....	48
2.7 地下水流数値解析モデル .....	53
3. WASTEF のホットセルでのガラス固化体の安全性試験 .....	59
3.1 放射性ガラス試料の調製 .....	60
3.2 ガラススラリーを含む冷却水の再利用システムの開発 .....	65
3.3 HLW ガラスによる金属表面の汚染に関する予備試験 .....	67
3.4 キャニスタ内の核廃棄物ガラスからのセシウムの揮発 .....	70
3.5 返還廃棄物の特性 .....	76
4. 高レベル廃棄物ガラス固化体用原子力施設の安全研究 .....	77

## Introduction

Research activities in the fiscal year of 1984 on high level waste management are reviewed following the progress reports (JAERI-M 82-145, 83-076, 84-133). Safety studies and development of new technologies were conducted on the national program.

The performances of waste forms were studied to assess the initial barrier against radionuclide release to environment from storage facilities and repository in deep underground.

SYNROC was studied as one of new technologies for the immobilization.

Durability of canister materials and mechanisms of retardation of nuclide migration in rock mass were studied in laboratories and field.

In order to carry out these studies the Waste Testing Facility (WASTE-F) has performed hot operation and field test in granite rock mass have been conducted.

### 1. Waste forms examination

H. Nakamura

Leaching behavior of waste forms were studied in order to assess the performance of the initial barrier to reduce the source term in geological disposal. The alteration of the surface of simulated waste forms leached in wet underground rock mass for one year were examined to estimate the leach rate in the environment of repository. The effect of devitrification on leaching of various elements was studied on relation with crystallized products.

Tensile strength of the glass was examined using specimens easily breakable to reduce the variation of measured values.

In order to know the leaching mechanism of SYNROC the leached surface was examined and origine of crystalline products on it were discussed. Cooperation between Japan and Australia on development of SYNROC waste forms started. Details of the preparation method were supplied and the trace experiments were carried out. Developments of apparatus for preparation of SYNROC specimen containing real waste were initiated.

## Introduction

Research activities in the fiscal year of 1984 on high level waste management are reviewed following the progress reports (JAERI-M 82-145, 83-076, 84-133). Safety studies and development of new technologies were conducted on the national program.

The performances of waste forms were studied to assess the initial barrier against radionuclide release to environment from storage facilities and repository in deep underground.

SYNROC was studied as one of new technologies for the immobilization.

Durability of canister materials and mechanisms of retardation of nuclide migration in rock mass were studied in laboratories and field.

In order to carry out these studies the Waste Testing Facility (WASTE-F) has performed hot operation and field test in granite rock mass have been conducted.

### 1. Waste forms examination

H. Nakamura

Leaching behavior of waste forms were studied in order to assess the performance of the initial barrier to reduce the source term in geological disposal. The alteration of the surface of simulated waste forms leached in wet underground rock mass for one year were examined to estimate the leach rate in the environment of repository. The effect of devitrification on leaching of various elements was studied on relation with crystallized products.

Tensile strength of the glass was examined using specimens easily breakable to reduce the variation of measured values.

In order to know the leaching mechanism of SYNROC the leached surface was examined and origine of crystalline products on it were discussed. Cooperation between Japan and Australia on development of SYNROC waste forms started. Details of the preparation method were supplied and the trace experiments were carried out. Developments of apparatus for preparation of SYNROC specimen containing real waste were initiated.



## 1.1 LEACHING BEHAVIOR OF SIMULATED HIGH-LEVEL WASTE GLASS IN GROUNDWATER

Hiroshi Kamizono

The purpose of the present work is to examine the leaching behavior of simulated high-level waste glass in actual groundwater in Japan. For the first stage of this purpose, in-situ burial tests were carried out by immersing the sample in groundwater coming through schalstein-type rock in the Akenobe mine in southwestern Japan. The results were compared with the laboratory test results obtained using synthesized groundwater and deionized water.

## Experimental

The simulated high-level waste glass used for the present study was borosilicate glass containing 11.7 wt% simulated high-level waste.

The glass specimens of 1 x 1 x 1 cm in size were subjected to three kinds of leach test.

Case 1: An in-situ burial test in which the specimens were immersed in actual groundwater in the Akenobe mine, Japan, for up to 1 year. The temperature of the groundwater was about 14°C.

Case 2: A static leach test in which the specimen was immersed in about 50 ml of synthesized groundwater at room temperature ( $20^{\circ}\text{C} \pm 5^{\circ}\text{C}$ ) for 1 year. The composition of the synthesized groundwater is given in Table 1.

Case 3: A static leach test in which the specimens were immersed in about 50 ml of deionized water at room temperature ( $20^{\circ}\text{C} \pm 5^{\circ}\text{C}$ ) for up to 1 year.

Scanning electron microscopy with energy dispersive X-ray analysis (SEM-EDX) was used for measuring the extent of leaching of the specimen. This technique was described in the previous paper [1]. The surface analysis by SEM-EDX was carried out in the above three cases. The concentrations of Na and Cs in leachates were measured by atomic absorption spectroscopy (AAS) in cases 2 and 3.

### Results and Discussion

Figure 1 shows the scanning electron microphotographs of the surface of the unleached specimen and of the specimens leached in three kinds of leachant for 1 year. In the cases of actual groundwater (Fig.1(b)) and synthesized groundwater (Fig.1(c)), many grooves occur on the surface of the leached specimens, indicating that some parts of simulated high-level waste glass dissolve more easily than others. On the other hand, in the case of deionized water (Fig.1(d)), such grooves are not observed, which means that leaching is progressing more uniformly than in cases 1 and 2.

The amount of Na ( $C/C_0$ -value) on the surface of the specimens is listed in Table 2. The  $C/C_0$ -value is defined as the ratio of the concentration of Na on the surface of a leached specimen ( $C$ ) to the initial concentration of Na before leaching ( $C_0$ ). The  $C/C_0$ -values for the specimens leached in actual groundwater (case 1) and synthesized groundwater (case 2) for 1 year are 0.92 and 0.91, respectively. On the other hand, the  $C/C_0$ -value for the specimen leached in deionized water (case 3) for 1 year is 0.76, which is smaller than the above values for actual groundwater and synthesized groundwater.

Figure 2 shows the relationship between the amount of Na on the surface of the specimen ( $C/C_0$ ) and the amount of Na in the leachates ( $NL_{Na}$ ) in cases 2 and 3 [1]. The value of  $NL_i$  is defined as what is called normalized elemental mass loss for the element  $i$  [2]. Although only one point was obtained in case 2, it is found in Fig.2 that the value of  $NL_{Na}$  for case 2 is larger than that for case 3 at a fixed  $C/C_0$ -value. This may be accounted for by the fact that many grooves were observed with the specimen leached in synthesized groundwater for 1 year (Fig.1(c)). In other words, the formation of many grooves may cause a higher leach rate than expected from the SEM-EDX observations. (See Table 2, which shows that the values of  $NL_{Na}$  and  $NL_{Cs}$  for the specimen leached in synthesized groundwater for 1 year are rather higher than those for the specimen leached in deionized water for 1 year.)

In conclusion, the SEM-EDX observation suggested that the extent of leaching of simulated high-level waste glass in actual groundwater and synthesized groundwater was smaller than that in deionized water. However, in the cases of actual groundwater and synthesized groundwater, partial leaching, which caused the grooves on the surface of specimens, should be taken into account. The formation of many grooves may cause a higher leach rate than expected from the SEM-EDX observation.

#### Reference

- [1] H.Kamizono and T.Banba, Report JAERI-M 84-220 (Japan Atomic Energy

Research Institute, Tokai, Ibaraki, 1984)

[2] D.M.Strachan, R.P.Turcotte and B.O.Barnes, Nucl. Technol. 65 (1982) 306.

Table 1 Value of pH and composition of synthesized groundwater

pH	7.7
Na	25.5 mg/l
Ca	120 mg/l
Mg	108 mg/l
HCO <sub>3</sub> <sup>-</sup>	Nearly saturated
SO <sub>4</sub> <sup>2-</sup>	380 mg/l

Table 2 The values of C/C<sub>0</sub>, NL<sub>Na</sub> and NL<sub>Cs</sub>

Sample (Leach time)	Sodium		Cesium
	C/C <sub>0</sub> -value*	NL <sub>Na</sub> ** (g/cm <sup>2</sup> )	NL <sub>Cs</sub> ** (g/cm <sup>2</sup> )
Case 1 (6 months)	0.93±0.03	—	—
Case 1 (1 year)	0.92±0.05	—	—
Case 2 (1 year)	0.91±0.03	1.6 × 10 <sup>-4</sup>	1.5 × 10 <sup>-4</sup>
Case 3 (3 months)	0.93±0.03	2.7 × 10 <sup>-5</sup>	ND
Case 3 (6 months)	0.92±0.03	3.9 × 10 <sup>-5</sup>	ND
Case 3 (1 year)	0.76±0.04	1.3 × 10 <sup>-4</sup>	8.7 × 10 <sup>-5</sup>

\* The C/C<sub>0</sub>-value of Na was shown with its standard deviation.

\*\* NL<sub>Na</sub> and NL<sub>Cs</sub> represent normalized elemental mass losses for Na and Cs, respectively. The concentrations of Na and Cs in leachates were measured by atomic absorption spectroscopy in cases 2 and 3. ND: Not detected. In case 1, leachates (actual groundwater) could not be collected.

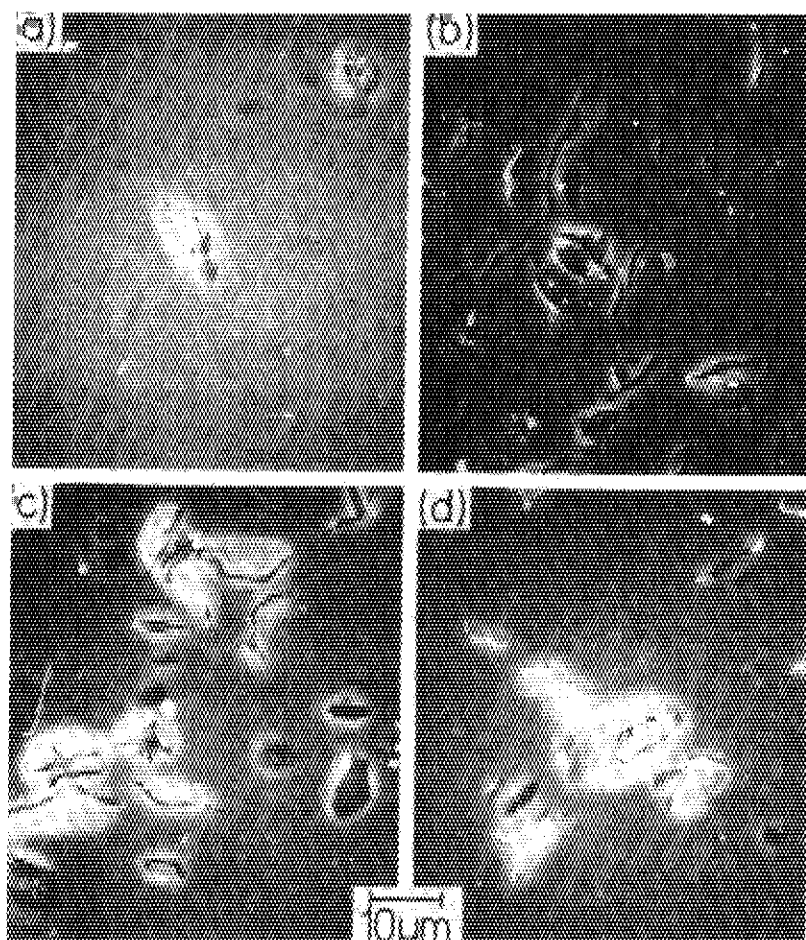


Fig.1. Scanning electron microphotographs of the surface of the unleached specimen (a) and the surface of the specimens leached in actual groundwater (b), in synthesized groundwater (c) and in deionized water (d) for 1 year.

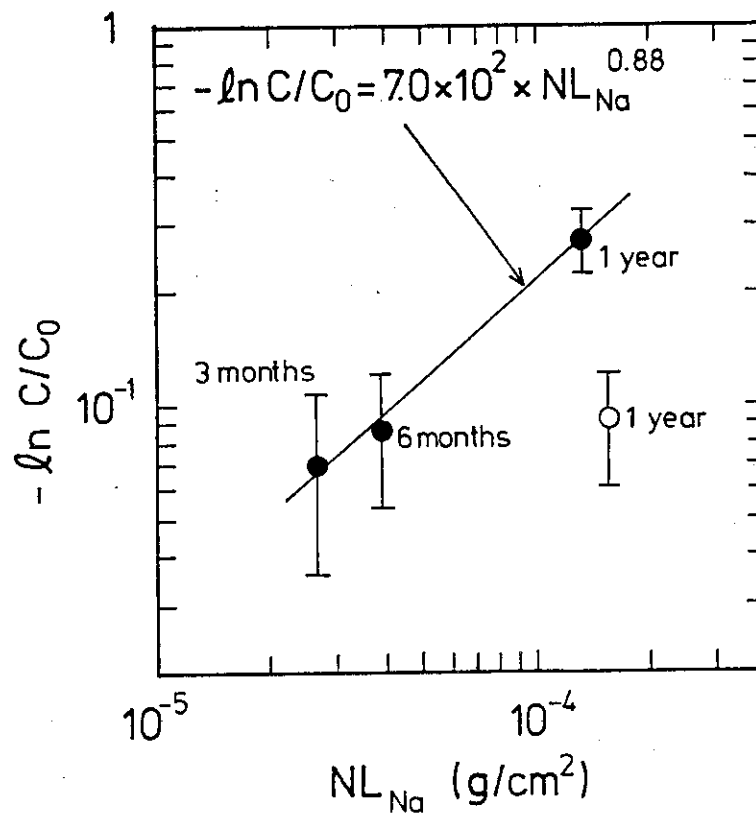


Fig.2 The relationship between  $-\ln C/C_0$  and  $NL_{Na}$ . ●: In the case of deionized water. ○: In the case of synthesized groundwater.

## 1.2 Soxhlet leach test of a devitrified simulated high-level waste glass

H. Mitamura

## Introduction

The nuclear waste glass can transform into various kinds of crystalline phases at elevated temperature. This phenomenon affects leaching which is a primary factor in establishing long term stability of the waste glass. The characteristics of the crystalline phases as well as the glass matrix in the devitrified waste glass need to be investigated from the standpoint of leaching. In the present report, Soxhlet leach test was carried out for a devitrified borosilicate glass containing simulated high-level waste (HLW) oxides.

## Experiment

A HLW glass was composed of 20 wt% of simulated HLW oxides and 80 wt% of glass additives<sup>(1)</sup>. The devitrified HLW glass was prepared by keeping at 750 °C for 1000 h<sup>(2)</sup>. As samples of leach test, a couple of about 5 mm cubes were cut out from the devitrified and the as-prepared HLW glasses, respectively. All surfaces of these samples were polished by hand on a lap with diamond paste. The samples were cleaned by a 3-minute ultrasonic wash in deionized water and then by three 3-minute ultrasonic washes in fresh absolute ethanol. The samples were dried at 110 °C and weighed.

Leach test was conducted for two months using modified Soxhlet extractor made from silica glass (Figure 1). About 50 ml of leachates

were collected at irregular intervals. Leachate compositions were analyzed with atomic absorption and inductively coupled plasma atomic emission spectroscopies. Analysis for Na and Cs was carried out with the former method and that for B, Mo, Sr, Ba, Cr and Fe was performed with the latter method.

### Results and discussion

Seven crystalline phases were newly formed by devitrification in addition to two phases, (Ru, Rh) $O_2$  and (Pd, Rh, Te), which had already occurred in the as-prepared HLW glass: (RE)BSi $O_5$ , Ce $O_2$ , Si $O_2$ , (RE)PO $_4$ , (Sr, Ba, RE)MoO $_4$ , an unknown phase rich in Si, Cr and RE, and the other unknown phase rich in Ni and Cr, where RE stands for rare earth elements<sup>(2)</sup>.

Figure 2 shows the leach rate of Na with time. Each of symbols in this figure indicates the average of two values for the two samples of each of the two kinds of HLW glasses. Both the devitrified and the as-prepared HLW glasses show constant leach rates of Na in early stages of the leach test. The averages of these constant leach rates of Na are  $6.1$  and  $2.1 \times 10^{-3}$  g/cm $^2$ d for the devitrified (till 11 days) and the as-prepared (till 7 days) HLW glasses, respectively. This indicates that glass matrix dissolution rate of the devitrified HLW glass is about three times higher than that of the as-prepared HLW glass. Subsequently the leach rates of Na for the devitrified HLW glass decrease more steeply than that for the as-prepared HLW glass.

Figure 3 shows relative leach rates on the basis of leach rates of Na. This figure reveals that in the as-prepared HLW glass the



leaching behavior of B is the same as that of Na. In this glass, the averages of the relative leach rates of Mo and Cs are, respectively, 1.16 and 0.8 all through the test period. The relative leach rate of Cr is constant nearly through the period. The relative leach rates of Sr and Ba vary widely and decrease gradually.

In the devitrified HLW glass, the leaching behavior of B is the same as that of Na nearly through the test period. The relative leach rate of B however decrease at the end of the test period. This implies that as the result of leaching of a considerable amount of B, the characteristics of  $(\text{RE})\text{BSiO}_5$  have become apparent:  $(\text{RE})\text{BSiO}_5$  is hard to be attacked by water. A significant decrease in relative leach rates of Sr and Ba by devitrification indicate that  $(\text{Sr}, \text{Ba}, \text{RE})\text{MoO}_4$  is difficult to be leached out. Komarneni et al.<sup>(3)</sup> has also said that  $\text{SrMoO}_4$  is highly stable in deionized water and other solutions. As a result of formation of  $(\text{Sr}, \text{Ba}, \text{RE}) \text{MoO}_4$ , the relative leach rate of Mo is smaller after devitrification than before that. It is however thought that a considerable amount of Mo still remained in the glass matrix of the devitrified glass because the stoichiometric amount of Mo was more than those of Sr and Ba. The relative leach rate of Cr is almost unchanged by devitrification. The leaching behavior of crystalline phases containing Cr is not clear.

#### References

- (1) H. Mitamura et al. Segregation of the elements of the platinum group in a simulated high-level waste glass. Nucl. and Chem. Waste Management, vol. 4, pp. 245-251 (1983).

(2) H. Mitamura, T. Murakami and T. Banba. Crystalline phases in a devitrified simulated high-level waste glass containing the elements of the platinum group. (under submitted).

(3) S. Komarneni, R. Roy and D. M. Roy. Evaluation of  $\text{SrMoO}_4$  in repository simulating tests. Nucl. Thech., vol. 62, pp. 71-74 (1983).

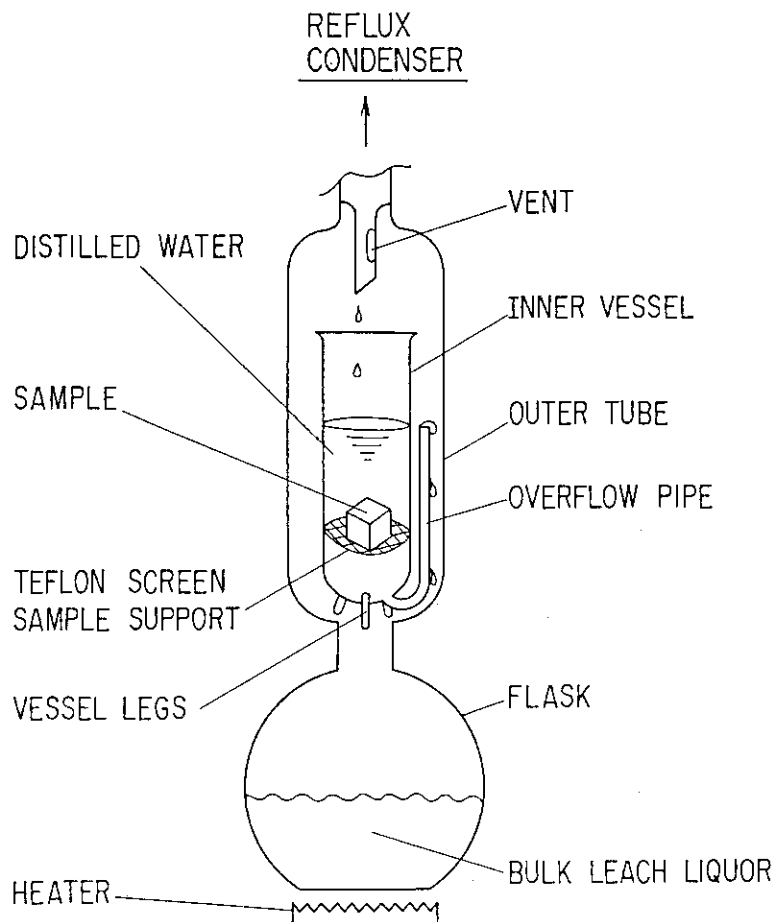


Fig. 1 A modified Soxhlet extractor for leach test

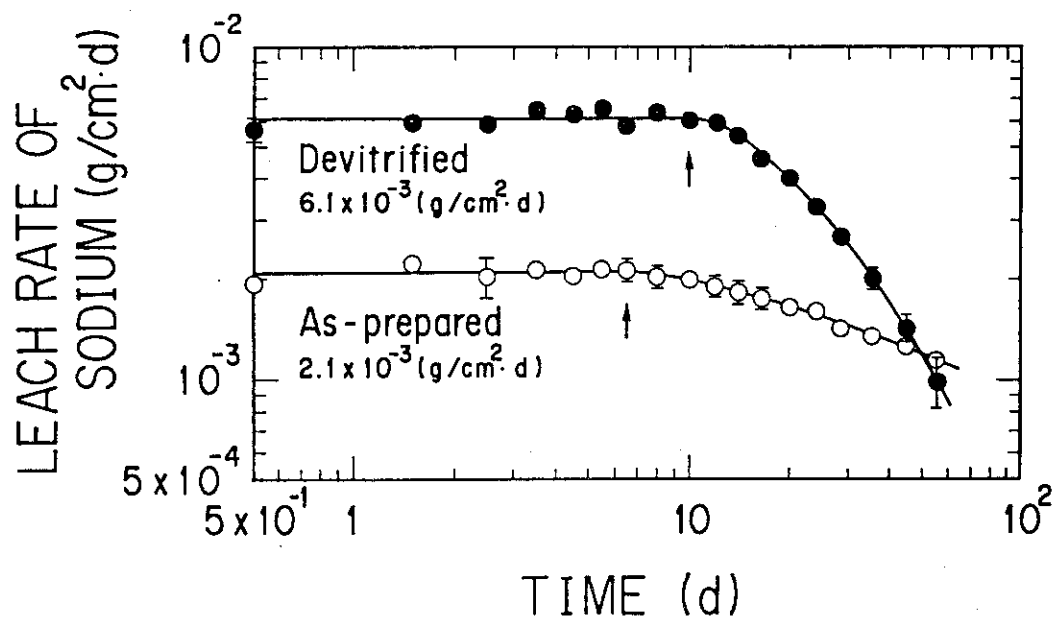


Fig. 2 Leach rate of sodium

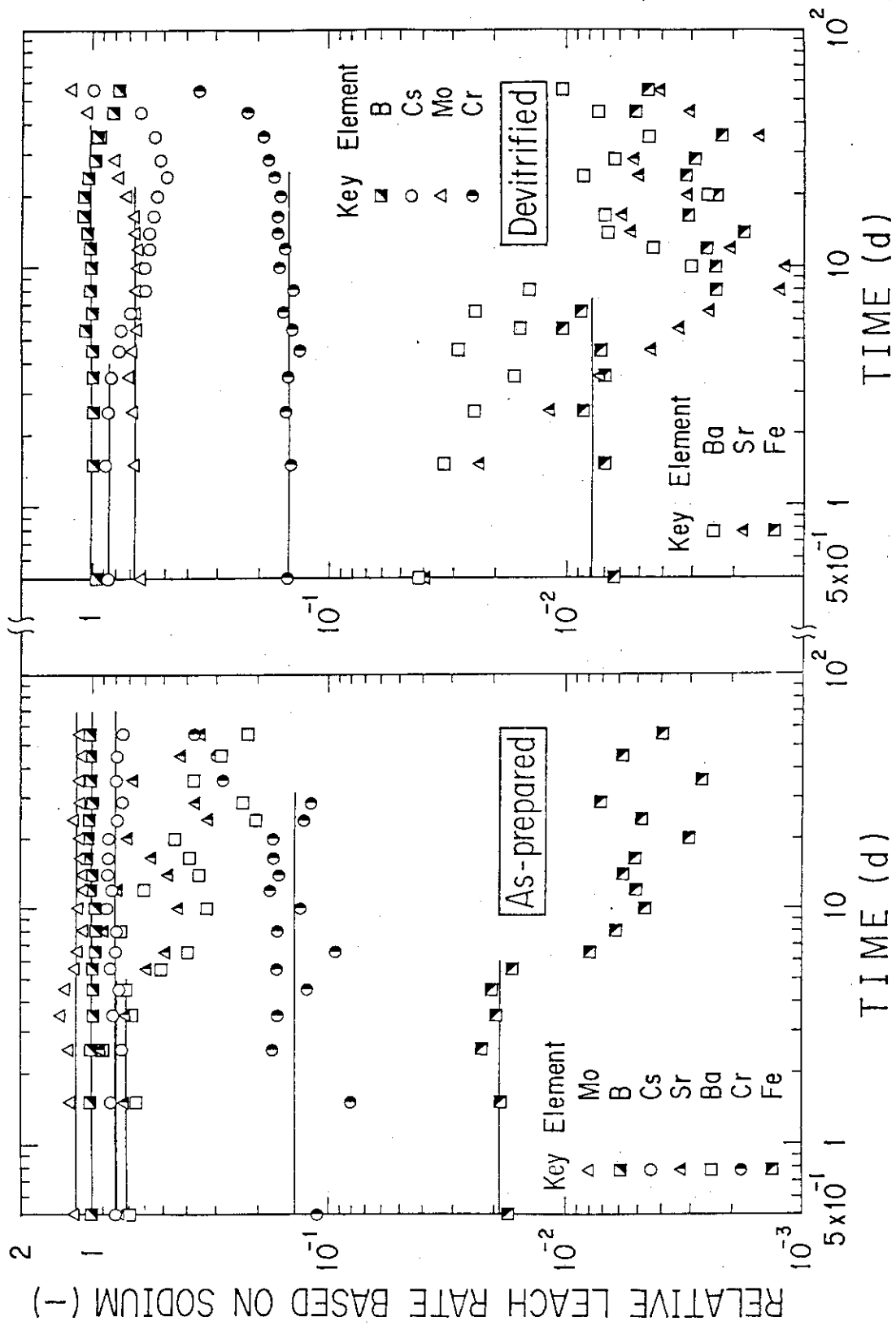


Fig. 3 Relative leach rates on the basis of that of sodium

### 1.3 Tensile Strength of Simulated High-Level Waste Glass

Hiroshi Kamizono

An important property expected from nuclear waste glass is high tensile strength since the thermal shock resistance of the glass is basically related to its tensile strength<sup>(1)(2)(3)</sup>. In the present note, the tensile strength of simulated high-level waste glass, the composition of which is the same as that used in our previous work<sup>(1)(2)</sup>, is examined. In addition, test specimens are designed with centers that would tend to be broken by tensile stress.

#### Experimental

The sample used for this study was borosilicate glass containing 14 wt% of simulated high-level waste. Through a vitrification process, square bars of the glass of 10 x 10 x 100 mm were prepared (Fig.1). Each bar was cut into three pieces and polished, q.v., A, B and C in Fig.1, and then the three pieces were welded by a flame into one specimen. Then, the central part of the specimen was half-melted, and drawn out by hand so that its center thinned down to about 1 mm in diameter.

#### Results and Discussion

Eight test specimens were made, six of which were broken at their centers during the measurements. Therefore, the intention that the test specimens break at their centers was successfully accomplished. The results for the six specimens, the centers of which were broken, are given in Table 1. As can be seen in Table 1, the values of the

tensile strength ( $S_t$ ) fall in a wide range of  $0.38 \text{ kg/mm}^2$  to  $6.2 \text{ kg/mm}^2$ . The measured  $S_t$ -values tend to be lower than expected because of a difficulty of eliminating bending moments during the measurements<sup>(4)</sup>. The lowest three  $S_t$ -values of 0.38, 0.50 and  $0.51 \text{ kg/mm}^2$  listed in Table 2 may have occurred as a result of such a difficulty. Although this difficulty seems to be inevitable in our tensile tests, the measured  $S_t$ -values are still useful as described below.

The maximum value of the measured tensile strength can be used for the estimation of the thermal shock resistance of the glass where the elimination of bending moments during tensile tests is difficult<sup>(3)</sup>. When the maximum value of  $6.2 \text{ kg/mm}^2$  obtained above is used, the threshold temperature difference ( $\Delta T_{th}$ ) for crack initiation observed in quench tests is calculated to be about  $79^\circ\text{C}$  by the following equation<sup>(5)</sup>,

$$\Delta T_{th} = S_t(1 - \mu)/E\alpha \quad (1)$$

where  $S_t$  is the tensile strength ( $6.2 \text{ kg/mm}^2$ ),  $\mu$  is Poisson's ratio (0.25),  $E$  is Young's modulus ( $7.56 \times 10^3 \text{ kg/mm}^2$ ), and  $\alpha$  is the thermal expansion coefficient ( $7.8 \times 10^{-6}/^\circ\text{C}$ ). The calculated value of  $\Delta T_{th}$  of  $79^\circ\text{C}$  obtained above is in good agreement with the experimentally observed value of  $74^\circ\text{C}$  determined by water quench tests<sup>(1)</sup>.

From the results obtained, it is concluded that the tensile strength of simulated high-level waste glass can be measured by the method presented here, and that the maximum value of the measured

tensile strength can be used for the calculation of  $\Delta T_{th}$ .

#### REFERENCES

- (1) KAMIZONO, H., SENOO, M.: Nucl. Chem. Waste Manage.: 4, 329 (1983).
- (2) KAMIZONO, H., NIWA, K.: J. Mater. Sci. Letters: 3, 588 (1984).
- (3) KAMIZONO, H., KIRIYAMA, Y.: J. Nucl. Mater., in press.
- (4) KOMEYA, K., HASHIMOTO, H.: Ceram. Japan, 11, 935 (1976).
- (5) KINGERY, W.D., BOWEN, H.K., UHLMANN, D.R.: "Introduction to Ceramics", (1976), John Wiley & Sons, New York.

Table 1 Results of the tensile tests

Number	D(mm)	L(kg)	$S_t$ (kg/mm <sup>2</sup> )
1	1.139	0.52	0.51
2	0.835	0.21	0.38
3	1.153	6.50	6.2
4	0.918	0.33	0.50
5	0.716	2.08	5.2
6	0.954	3.63	5.1

D: the minimum diameter at the center of the specimen.

L: the maximum load applied to the specimen.

$S_t$ : the tensile strength of the specimen ( $= 4L/\pi D^2$ ).

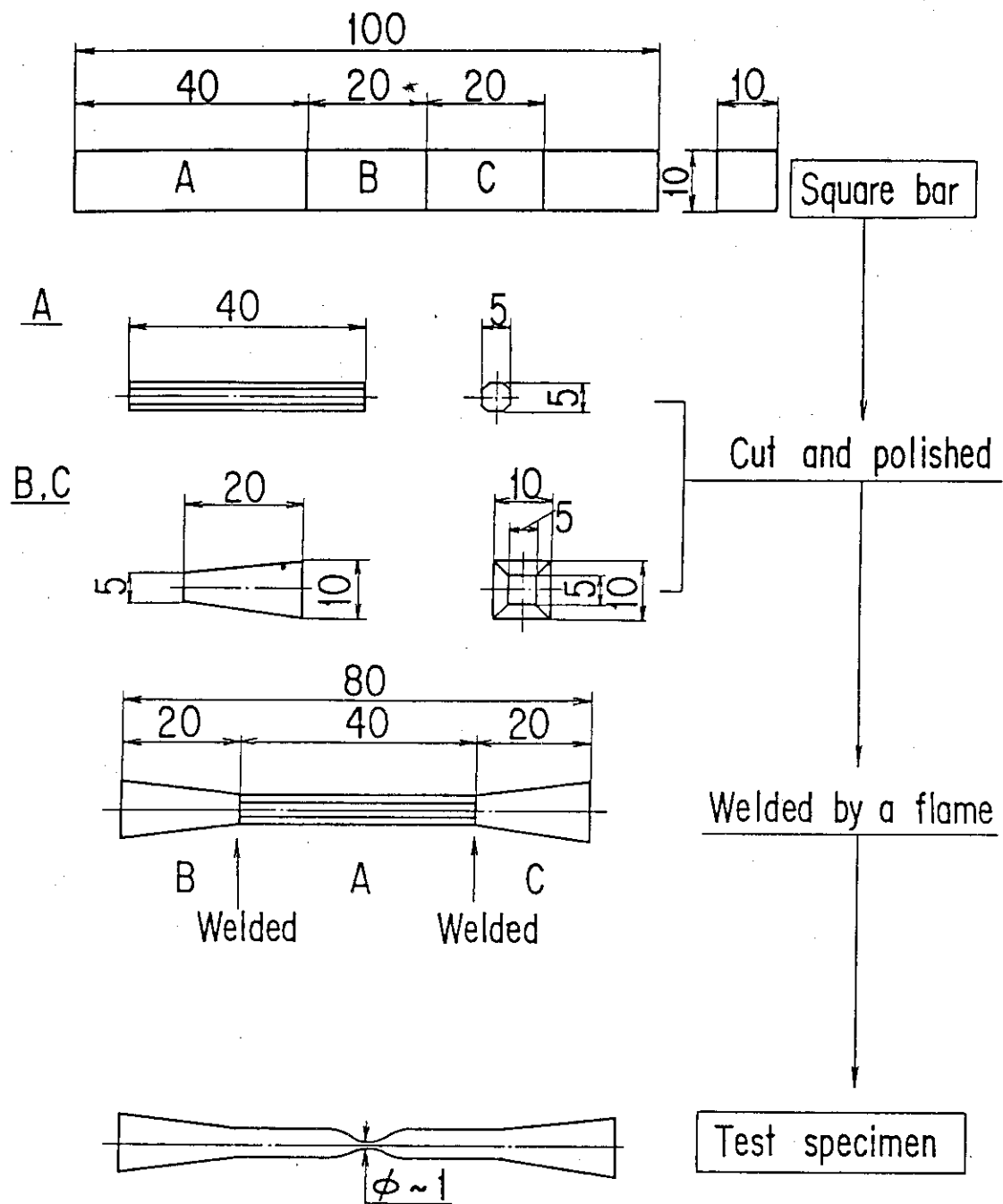


Fig. 1 Procedure for preparation of the test specimens (All dimensions are given in mm.)



#### 1.4 Crystalline product on surface of SYNROC after long leaching

T. Murakami

### 1. Introduction

The long-term leach rates, which are indispensable data for the safety evaluation of high level waste disposal, can be predicted on the basis of the leaching mechanisms of high level waste forms. Murakami and Banba identified a crystalline product in surface layers through the leaching study of a glass waste form [1] and they pointed out importance of the role of the crystalline product in the leaching mechanisms [2]. It is also expected that crystalline products must have an influence on the leaching mechanisms of ceramic waste forms though the mechanisms are still poorly understood. Ryerson et al. [3], Clarke et al. [4] and Jantzen et al. [5] found crystalline products on surface of their ceramic waste forms other than SYNROC-C [6]. The present leaching experiment on SYNROC-C has shown different results from those by the above authors.

### 2. Experimental procedures

The SYNROC-C sample was synthesized with hot isostatic press at 1200°C and 800 kg/cm<sup>2</sup> for one hour in an atmosphere of argon. The fabrication of the sample was mentioned in detail along with the composition in the previous paper [7]. Two fractured specimens of

about 3 mm in diameter were subjected to leach test with a modified Soxhlet type at 100°C; they were leached for 10 days and 300 days. Leaching solution flowed continuously through the sample chamber of a Soxhlet apparatus at a rate of about 100 cm<sup>3</sup>/h. Surfaces of the specimens before and after leaching were observed by scanning electron microscopy equipped with energy dispersive X-ray spectroscopy (SEM-EDX).

### 3. Results and discussion

Figure 1 shows the scanning electron micrographs of the surfaces of the specimens before and after leaching. Morphological change of the surface does not occur significantly after 10 day leaching (Fig. 1B) but occurs after 300 day leaching (Figs. 1C and 1D). New crystals are formed and concentrate on a part of the surface of the specimen; the size of the crystals is usually about 1 micrometer in length (Fig. 1C) and on one area of the surface, the crystals longer than 20 micrometers are also observed (Fig. 1D). The SEM-EDX analysis revealed that the crystals contain only aluminum except 0.6 wt% TiO<sub>2</sub>, which we hereafter call phase A (Fig. 2).

An X-ray diffraction method did not give an effective result for identification of phase A. Because of high concentration of aluminum in phase A and medium contrast of phase A in the SEM image, phase A can be aluminum hydroxide or aluminum oxide. Out of the two, aluminum hydroxide is possibly formed under the present leaching conditions similar to those of the other studies in which aluminum

hydroxide was found [3,4,5].

The present leach test was carried out at a high flow rate [8], therefore the formation of phase A must not result from reprecipitation from the leaching solution. Since aluminum in the present SYNROC-C sample is accommodated in aluminum-containing phases, magnetoplumbite and hollandite [7], the formation of phase A is probably related to decomposition of magnetoplumbite and/or hollandite. Hollandite contains 66%  $\text{TiO}_2$ , 25%  $\text{BaO}$  and 6%  $\text{Al}_2\text{O}_3$  [7], and Ti and Ba are the elements difficult to leach into solution [9]. Accordingly, if the formation of phase A would result from decomposition of hollandite, for example, by a reaction,  $\text{BaAl}_2\text{Ti}_6\text{O}_{16} + \text{CO}_2 + \text{H}_2\text{O} = \text{BaCO}_3 + 6\text{TiO}_2 + 2\text{AlO(OH)}$  [10], we could find Ti rich areas or Ba rich areas. However we found neither Ti rich areas nor Ba rich areas on the surface of the specimen after leaching. Therefore the formation of phase A may not be related to decomposition of hollandite.

Although no direct evidence was observed for decomposition of magnetoplumbite, there are two facts which support that the formation of phase A results from decomposition of magnetoplumbite. First, magnetoplumbite contains 84.5%  $\text{Al}_2\text{O}_3$  and the amounts of the other components are small: 8.4%  $\text{TiO}_2$ , 4.5%  $\text{Fe}_2\text{O}_3$  and 2.5%  $\text{CaO}$  [7]. Accordingly, if magnetoplumbite would be decomposed, aluminum could be always found and the other elements could not be necessarily found. This is consistent with the result that phase A was found on the surface after leaching but other phases such as a titanium-rich phase were not found. Second, Troester et al. suggested that aluminum

hydroxide is formed as a result of dissolution of magnetoplumbite [11].

Aluminum hydroxide was observed as a crystalline product in other leaching studies [3,4,5]. Ryerson et al. [3] studied leaching of SYNROC-D which consists of perovskite, zirconolite, spinel and nepheline, and reported that  $\text{Al}(\text{OH})_3$  polymorphs, gibbsite and bayerlite were found because of dissolution of nepheline alone. Clarke et al. [4] and Jantzen et al. [5] used nuclear waste ceramics which consist of magnetoplumbite, spinel, corundum and uraninite. They reported that dissolution of corundum and/or spinel were responsible for the formation of boehmite,  $\gamma\text{-AlO}(\text{OH})$ , but not that of magnetoplumbite. The constituent mineral phases of SYNROC-C are hollandite, perovskite, zirconolite and magnetoplumbite, which are different mineral assemblage from those of SYNROC-D or the nuclear waste ceramics. Aluminum hydroxides are formed as crystalline products due to decomposition of different mineral phases even if the mineral assemblages are different. This suggests different leaching mechanisms among SYNROC-C, SYNROC-D and the nuclear waste ceramics.

Further studies are required to elucidate the role of crystalline products in the leaching mechanisms of ceramic waste forms.

## References

- [1] T. Murakami and T. Banba, Nucl. Technol. 67 (1984) 419.
- [2] T. Banba and T. Murakami, Nucl. Technol. (in press) (1985).
- [3] F. J. Ryerson, F. Bazen and J. H. Campbell, J. Amer. Ceram. Soc. 66 (1983) 462.
- [4] D. R. Clarke, C. M. Jantzen and A. B. Harker, Nucl. Chem. Waste Manage. 3 (1982) 59.
- [5] C. M. Jantzen, D. R. Clarke, P. E. D. Morgan and A. B. Harker, J. Amer. Ceram. Soc. 65 (1982) 292.
- [6] A. E. Ringwood, S. E. Kesson, N. G. Ware, W. O. Hibberson and A. Major, Geochem. J. 13 (1979) 141.
- [7] T. Murakami, Nucl. Chem. Waste Manag. (in press) (1985).
- [8] D. M. Strachan, in: Advances in Ceramics vol. 8, Eds. G. G. Wicks and W. A. Ross, (The American Ceramic Society, Inc. Columbus, Ohio, 1984) p.12.
- [9] T. Murakami, T. Banba and H. Nakamura, submitted to Nucl. Technol.
- [10] R. L. Segall, S. Myhra, R. St. C. Smart and P. S. Turner, Report NERDDC Project No 80/0049 (Griffith University, Brisbane, Queensland, 1984).
- [11] J. W. Troester, W. P. Freeborn and W. B. White, in: Advances in Ceramics vol. 8, Eds. G. G. Wicks and W. A. Ross (The American Ceramic Society, Inc. Columbus, Ohio, 1984) p.247.

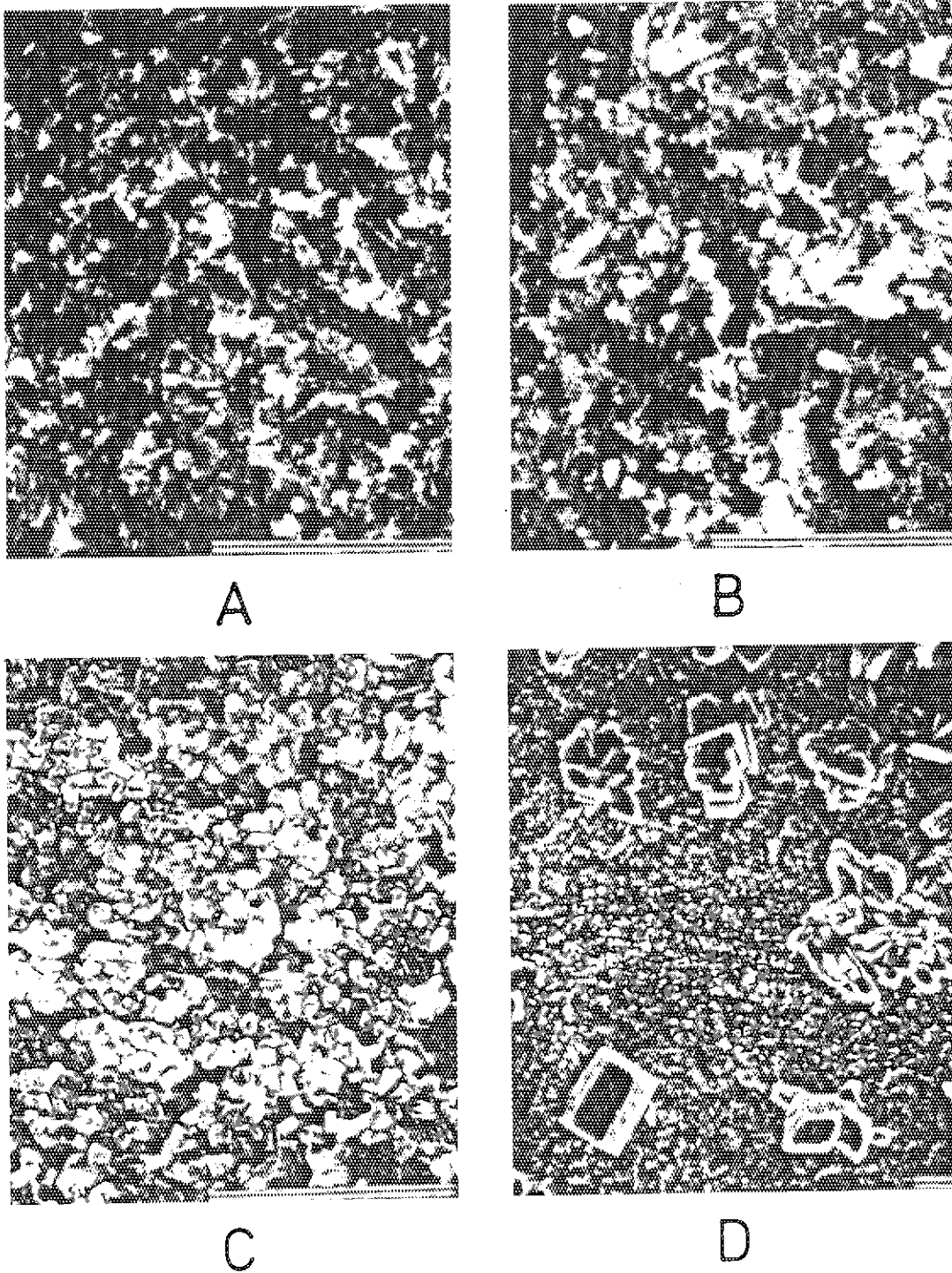


Fig. 1 Scanning electron micrographs of surfaces of SYNROC-C specimens; (A) before leaching, (B) after 10 day leaching, (C) after 300 day leaching without large crystals of phase A, and (D) after 300 day leaching with large crystals of phase A. Bars represent 10 micrometers.

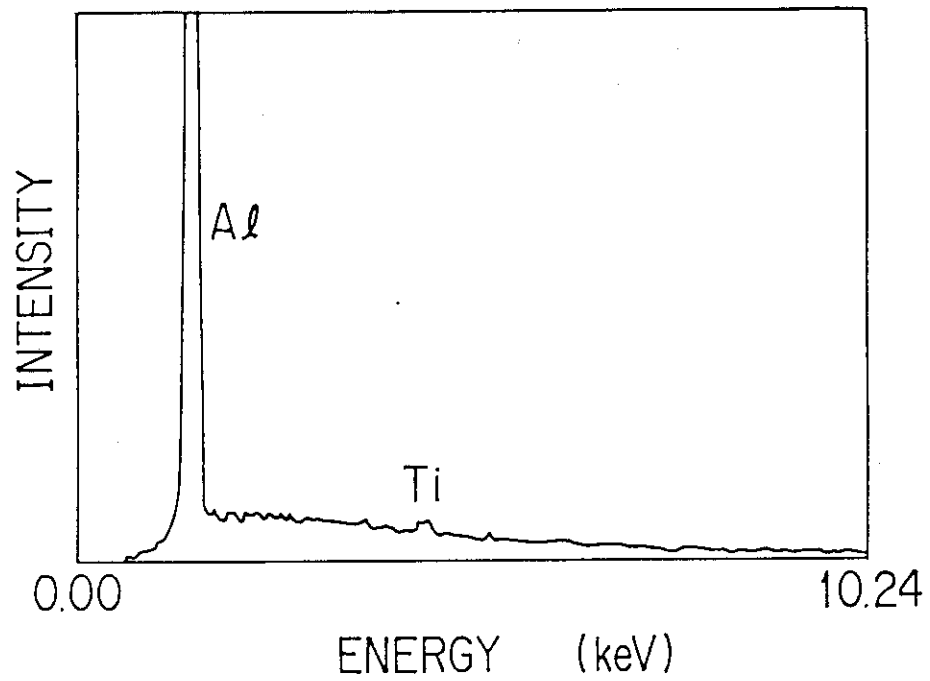


Fig. 2      Energy spectrum of phase A.

## 2. Safety evaluation for geological disposal

H. Nakamura

Durability of the canister materials was studied by irradiation test in laboratory and heating experiments in-situ. U bent specimens of stainless steel, inconel, hastelloy and Ti-alloy were tested. These experiments will be continued for detail discussions.

Diffusions of radionuclides in buffer mass and rock were studied to assess the migration in near field. Combination of active carbon and bentonite was considered a candidate buffer material to retard the migration of Tc. The bentonite, which were stuffed for 2 years in a simulated disposal pit were taken out and the water content was measured.

The experiments in granite rock mass were progressed as the schedule. The heating test to obtain the fundamental data was finished and water flow tests in fracture zone and engineered barrier tests started. The hydrology data obtained in this test site was used for verification of JAERI codes and NRC codes, which is one of the cooperation program. 3D-SEEP developed in JAERI was tested in HYDROCOIN project.

### 2.1 Diffusion of radionuclides into rock

H. Nakamura and S. Muraoka

Retardation factors by chemical adsorption of nuclides have been studied as the function of barrier by rock mass. Diffusion to rock mass and dilution by pore water is also important phenomena especially for radionuclides of low Kd values such as  $^{99}\text{Tc}$  and  $^{237}\text{Np}$  in oxidic groundwater.

We conducted diffusion tests immersing granite sticks into radioactive solutions last year. However, creep of radionuclides on surface and evaporation water were liable to make the diffusion complex. Therefore, we changed the system to measuring the diffusion of radioisotopes charged in the center of granite disk, which was immersed in water.

#### Experiment

Cored granite block was cut in 2 cm thick and small holes were drilled as shown in Fig. 1. The radioactive solutions were prepared by



evaporation to dryness of a few ml of acidic solution containing a few 0.1  $\mu\text{Ci}$  and dissolution of them with a few ml of distilled water. 0.1 ml of the solution was charged in the center hole, and other holes were filled with deionized water.

#### Result

Trace amount of  $^{90}\text{Sr}$  was detected in the hole at 2 mm.  $^{137}\text{Cs}$  and  $^{241}\text{Am}$  could not be detected. The distributions of  $^{95\text{m}}\text{Tc}$  and  $^{237}\text{Np}$  are shown in Fig. 2, respectively.

Glass spiked with  $^{244}\text{Cm}$  and  $^{238}\text{Pu}$  have been placed in the center hole and diffusion of the leached nuclides will be measured in WASTEF.

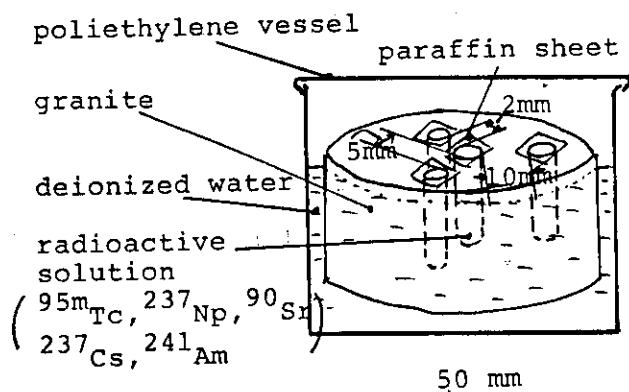


Fig.1 Schematic drawing of the diffusion experiment

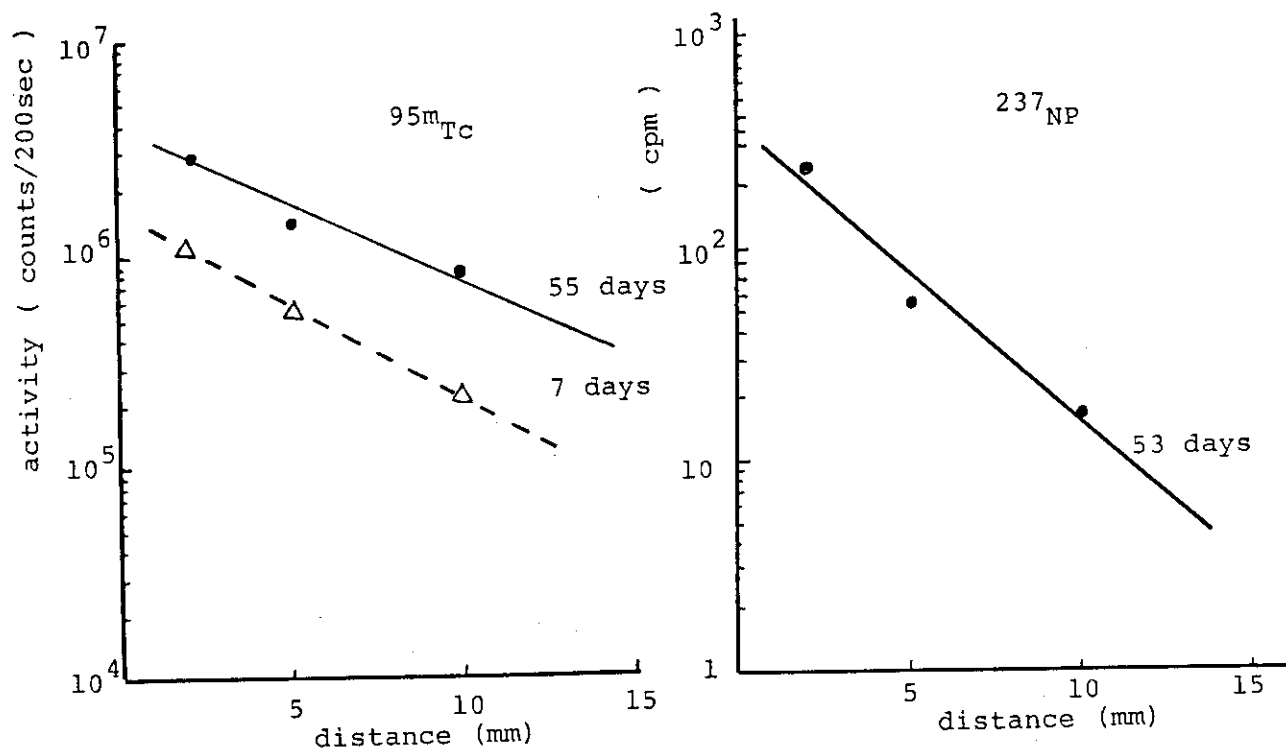


Fig.2 Distribution of radioisotopes after diffusion

## 2.2 Gamma-ray irradiation effects on near-field phenomena in geologic repositories for radioactive waste

M. KUMATA

### Introduction

In assessing the long-term integrity of an engineered geological repository, in particular a repository containing conditioned high level wastes (HLW), an understanding as to the potential causes of nuclides release and migration to the biosphere is necessary. The physical and chemical effects of heat and radiation from the waste are predominantly limited to the near-field. Chemical interactions at elevated temperature in the presence of radiation and water, have been studied in relation to corrosion, sorption, alteration of glass and rocks and their properties. The importance of the thermal and radiological effects on host rock, backfilling, waste package and the solidified waste is well recognised as also the aspects of corrosion, waste-rock interactions, diffusion, dispersion and sorption in the near-field.

The present study was planned to clarify the effect of gamma-ray irradiation on waste-water-rock interactions, leaching stability of glass and corrosion resistance of canister materials. Two series of gamma-ray irradiation test have been carried out. One is the test by use of single nuclide source of  $^{137}\text{Cs}$  and  $^{90}\text{Sr}$  in the hot cell of WASTEF. The other test has been carried out by use of spent fuel in JMTR.

## Experimental

### Materials

Granite and basalt were used as host rocks and borosilicate glass containing about 29 % of simulated nonradioactive high level waste was used as a vitrified waste form. Bentonite was used as one of candidate backfilling materials. Type 304 stainless steel and Type 309s stainless steel were used as the canister materials and Ti and Ticode were used as one of the overpack materials. Double U bent specimens of 1 mm thickness for stress corrosion cracking test were adopted (Fig. 1) for these metal materials. These solid materials were encapsuled in stainless steel capsul with three kind of solutions. The solutions used in this study were deionized water and two simulated ground water. These simulated groundwater were made from powdered granite and basalt by boiling down. The cation concentrations of the simulated groundwater were shown in Table 1. The combination of materials of specimens are listed in Table 2. Fig. 2 shows a schematic diagram of encapsuled specimens in a stainless steel capsul.

### Gamma-ray Irradiation

$^{137}\text{Cs}$  source of 2660 Ci and  $^{90}\text{Sr}$  source of 14700 Ci were used as single radioactive gamma-ray sources respectively in a hot cell of WASTE-F. Dose rate of  $^{137}\text{Cs}$  and  $^{90}\text{Sr}$  were  $6 \times 10^6$  R/h and  $2.2 \times 10^3$  R/h respectively. The stainless steel capsuls encapsuled specimens were arranged around the source in a granite container. Another gamma-ray source was spent fuel in JMTR. The capsuls were placed in the irradiation space of the spent fuel rack. Dose rates of the spent fuel were measured by using a ionization chamber and attenuation curves were described.

Sample temperatures rising from gamma-heat of each source were measured. The solutions were analyzed for their change after gamma-ray irradiation by atomic absorption spectrophotometry (AAS) and inductively coupled plasma atomic emission spectroscopy (ICP).

## Results

The apparent leaching ratio of Cs and Sr included in a simulated HLW glass which have been immersed in deionized water under irradiation during three months were  $4.19 \times 10^{-12}$  cm/sec and  $1.86 \times 10^{-12}$  cm/sec, respectively.

Concerning to stress corrosion cracking (SCC) on stainless steel, as already reported, under gamma-ray irradiation, it seems that the simulated groundwater delays SCC of stainless steel because of the existence of the leachant from rock sample. The pH value of the solutions with the stainless steel specimens increased in proportion to the dose because of the reaction between a stainless steel and oxidizing agents produced by radiolysis of solution<sup>(1)</sup>. Quartz consisting granite changed into purple to dark purple like black.

## References

- (1) JAERI M-84-133

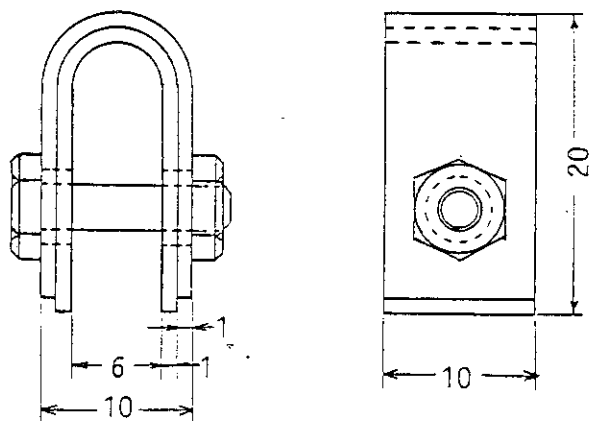


Fig.1 Double U-bend specimen (unit; mm)

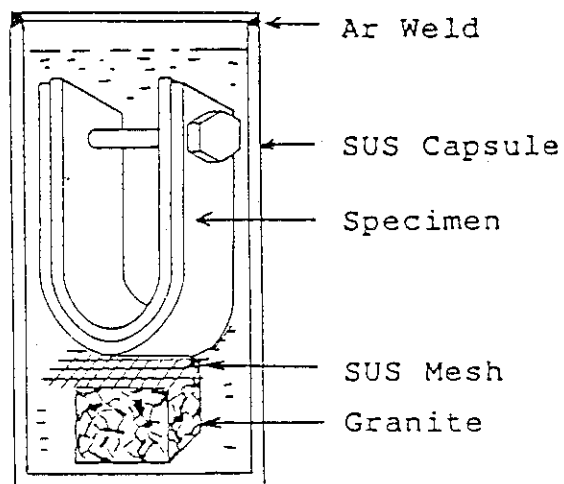


Fig. 2 Schematic diagram of a irradiated capsule with metal spesimen - granite - granite saturated water combination

Table 1 Cation concentrations of the  
simulated ground water ( ppm )

component	granite saturated water	basalt saturated water
Si	32.5	45.5
Al	5.08	5.24
Mg	0.51	2.51
Ca	3.98	5.91
Fe	7.19	4.45
Mn	0.04	0.17
Na	14.5	19.1
K	9.0	7.4
B	0.5	0.8
Ba	0.057	0.005
Mo	0.16	0.16
Cs	0.4	0.4
Sr	0.013	4.253

Table 2 The combination of specimens

No.	Specimens
1	SUS 304 - deionized water
2	SUS 309s - deionized water
3	SUS 304 - granite - granite saturated water
4	SUS 309s - granite - granite saturated water
5	SUS 304 - basalt - basalt saturated water
6	glass - granite - granite saturated water
7	glass - basalt - basalt saturated water
8	glass - deionized water
9	SUS 304 - bentonite
10	SUS 309s - bentonite
11	glass - bentonite
12	granite - bentonite
13	basalt - bentonite
14	Ti - deionized water
15	Ti - granite - granite saturated water
16	Ti - deionized water
17	Ti - granite - granite saturated water

## 2.3 Diffusion of ground water into buffer mass of a simulated disposal pit and research on buffer materials suitable for sorption of Tc

T. YANAGIDA

### Introduction

In the deep underground repository of High-Level Radioactive Waste (H.L.W.), it is required that the duration of waste packages have to be at least one thousand years. In this period, most of F.P. decays, but a few radionuclides which have a very long half life scarcely decay and remain highly radioactive.

After the failure of H.L.W. packages, leaching of H.L.W. starts. The radionuclides are dissolved into ground water and are diffused through buffer mass in the repository and geological formations. The ability to retard the diffusion of such radionuclides is expected in buffer mass and geological formations.

The distributions of water content in buffer mass which was stuffed in the simulated disposal pit were measured in order to investigate impermeability of buffer mass.

The distributions of  $\text{TcO}_4^-$  in bentonite mixtures which were composed with combinations of various materials were measured in order to research on buffer materials suitable for sorption of Tc.

### The diffusion of ground water into buffer mass of a simulated disposal pit

#### Experimentals

The simulated disposal pit was bored at a floor of the gallery in the metal mine located 380m below the surface. The leakage of water into the pit of which diameter and depth were 33cm and 3.3m respectively was 2600ml per 10 days. The pit was stuffed with bentonite (KUNIGEL VA) with a pipe in the centre of it. Every 25kg of bentonite powder was compacted by the pressure of 2 MPa, and its wet and dry densities were 1.27, 1.15 g/cm<sup>3</sup> respectively.



The water contents were measured at following three stages.

- 1). Initial stage. (before heating)
- 2). Heating stage. (just after heating)
- 3). Cooling stage. (two years after heating)

At each stage a vertical distribution of water contents in the bentonite was logged by a neutron scatter method. Just after the logging of cooling stage, the bentonite was dug out and the water contents of the bentonite were measured by weight loss with drying at the temperature of 110 °C.

## Results and discussions

The neutron count rates between the standard and the measurements were logged. The water contents of the bentonite at cooling stage were measured according to weight losses. The vertical distributions of water contents in the bentonite at each stage gained by fitting the line of the neutron rates and the line of the water contents is shown in Fig. 2.

The water content distribution in the bentonite at cooling stage showed two peaks located at the depth of 0.8 and 2.8 m from the gallery floor.

The locations of two peaks matched the locations of two of five fractures in the pit (Fig. 1). The moisture of highly wet area is considered to be supplied mainly from these two fractures. The domain of highly wet area extended to 60 and 70 cm respectively from each fracture. The ground water diffused through the bentonite at the velocity of 30 and 35 cm per year.

The total amount of water in the pit was 33.7% of that of the water leakage if the leakage continued at the same rate as initial one (260 ml/day).

## Research on buffer materials suitable for sorption of Tc

### Experimentals

A solution of  $^{95m}\text{TcO}_4^-$  of which initial radioactivity was 0.95  $\mu\text{Ci}/\text{ml}$  was used in this experiment.

The specimens of the buffer materials were the combinations of bentonite

, zircon sand, glass, magnetite and active carbon. The particle size of the materials except the bentonite was under #100 mesh and that of the bentonite was under #300 mesh. The materials and contents of each specimen are shown in Table 1.

Specimens were mechanically compacted in the stainless steel pipes with the pressure of 47MPa. The density of bentonite alone was  $1.99 \text{ g/cm}^3$ .

The solutions of 10 ml were added above the specimens in the pipes.

These pipes were kept in a moist circumstance for 56 days as shown in Fig. 3.

The specimens were cut to about 5mm disks. The vertical distributions of radioactivity of  $^{95}\text{Tc}$  in the specimens were obtained by using NaI scintillation counter for the disks.

## Results and discussions

A few milli-liter of solution remained above the specimens except the case of bentonite alone. All specimens were penetrated by the solution. The vertical distributions of  $\gamma$ -ray count rate in the specimens are shown in Fig. 4.

In the case of bentonite + zircon sand, bentonite + glass and bentonite + glass + magnetite, the distributions of radioactivity were uniform from top to bottom of the specimens. In the case of bentonite alone, the distribution showed the curve ranging one order between top and bottom.

In the case of bentonite + glass + zircon sand + active carbon, the range of the count rates spreaded two order. There was sufficient effects to retard the diffusion of  $\text{TcO}_4^-$  in the case of bentonite + glass + zircon sand + active carbon.

It is guessed that a active carbon may be a good absorber for  $\text{TcO}_4^-$ .

The velocity of diffusion in the case of bentonite alone was faster than other cases. This fact may derive from an effect of particle size of components in the specimens.

Table 1 Component and content of specimens

No.	Ben- tonite	Glass	Mag- netite	Zircon sand	Active carbon
1	100	—	—	—	—
2	20	—	—	80	—
3	20	80	—	—	—
4	20	35	—	40	5
5	20	40	40	—	—

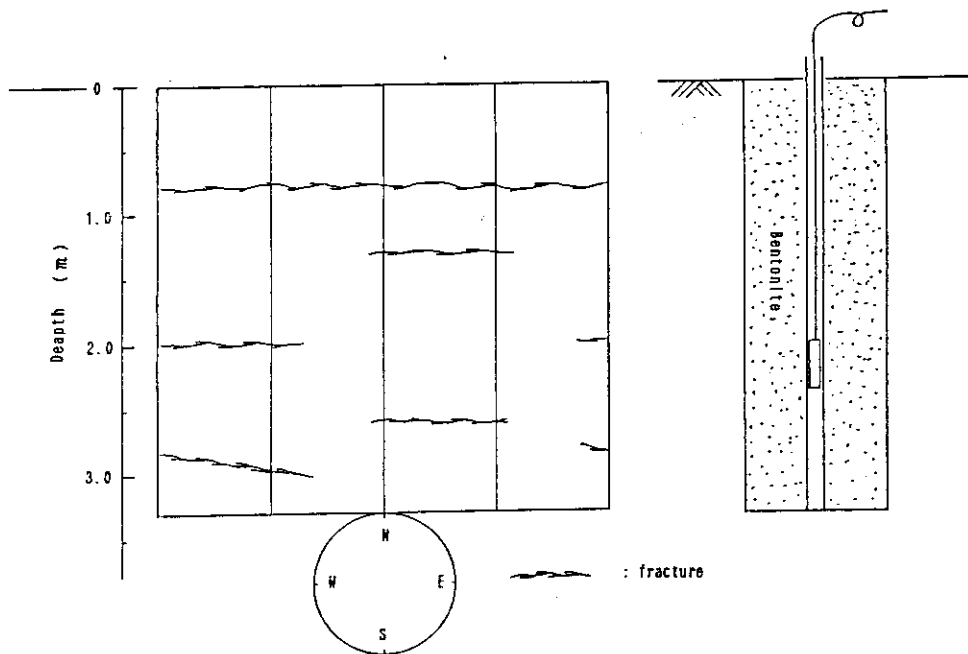


Fig. 1 The simulated disposal pit

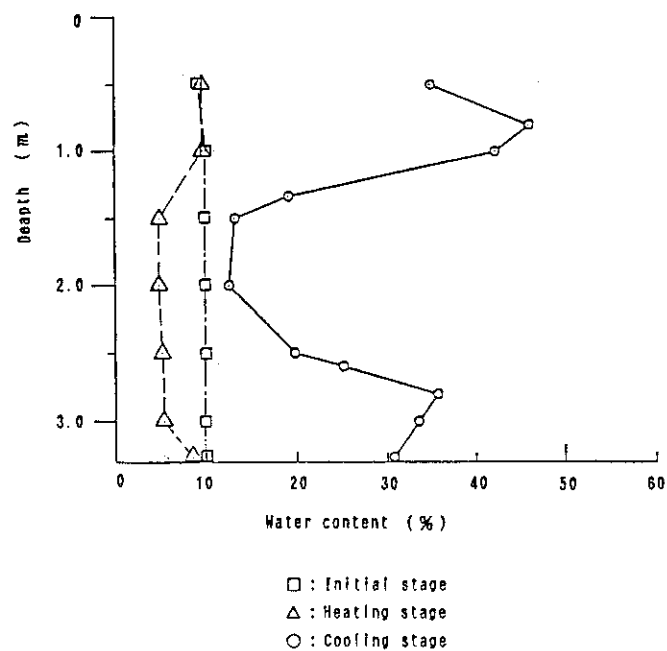


Fig. 2 Water contents of the bentonite

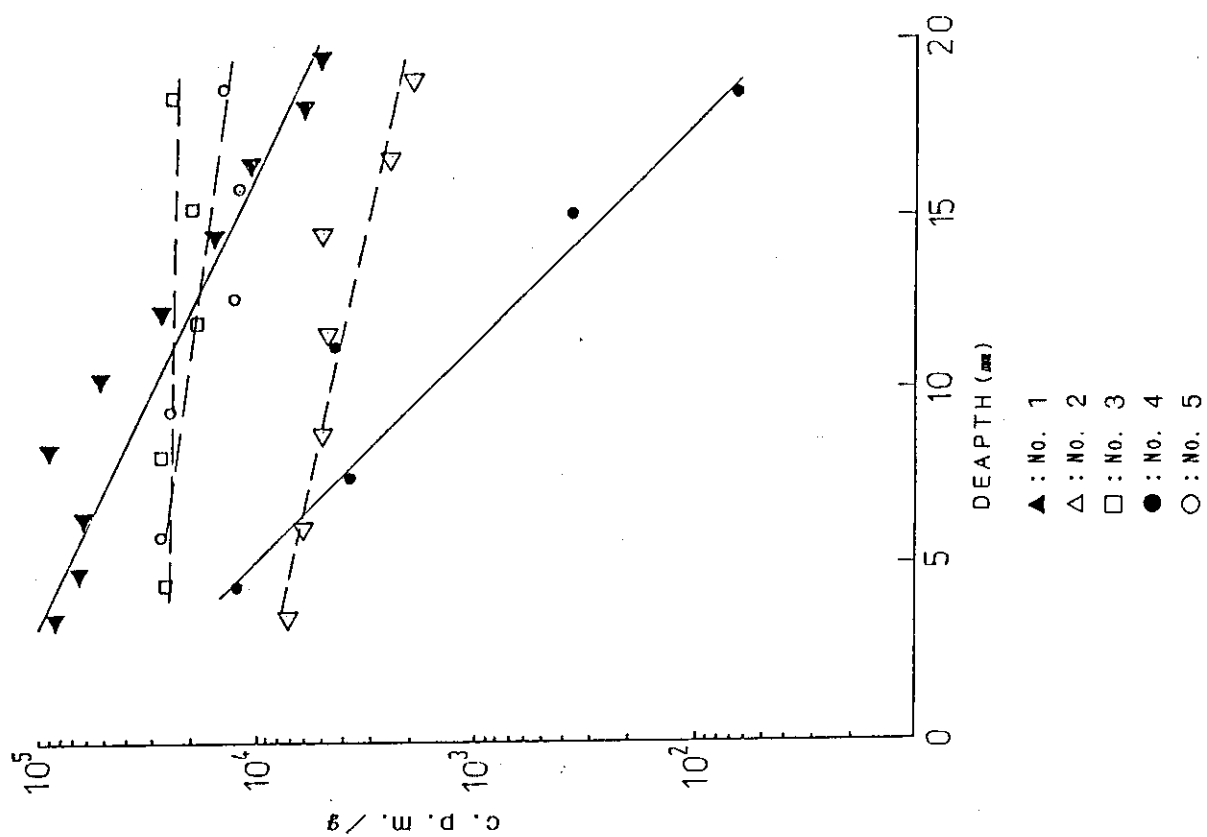


Fig. 4 Vertical distribution of  $T_c$

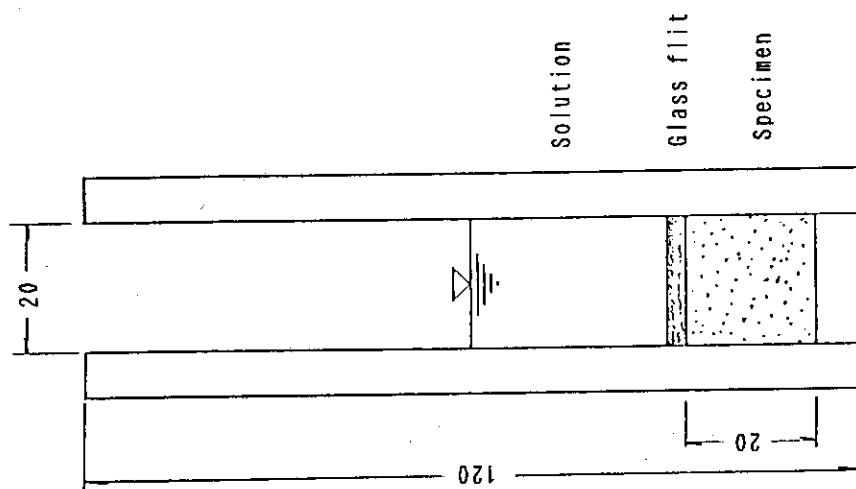


Fig. 3 Diffusion experiment

## 2.4 Progress with Field Experiments in Granite Rock Mass

K. Shimooka

### 1. Background

Over the past several years, the High Level Waste Management Laboratory has been involved in field experiments in deep mines which are in the complex formations of sedimentary rocks and metamorphic rocks. Results from the series of field experiments in such rock types suggest that a temperature isotherm around the wastes can be approximately estimated by thermal conductivities of the rocks. It was also revealed, however, that the waste migration in the rocks could hardly be estimated with laboratory data.<sup>1)</sup>

Another important rock is a granite for the selection of the disposal site. It is widely distributed in our country and is convenient for fundamental experiments because of its relatively simple and homogeneous nature. 3 year plan was made for series of tests in the granite which includes excavation of the experimental room, system performance tests and deep hole hydrological tests. The experimental place was chosen near JAERI. Experimental room is at a depth of 40 m below the surface. It is not very deep though, but has many advantages; easy to go, economical to excavate and satisfactory to the test. The primary objective of the tests is to establish the reliability of the measuring technology and also monitoring systems.

### 2. Characteristics of the granite

In order to compare the results from field experiments to those

of prediction with laboratory data, properties of the granite were measured. Density, specific heat and thermal conductivity were measured on specimens of the granite core from the experimental site. These values are listed in Table 1.

The rock at the experimental site is a condensed biotite-granite.

### 3. Heater Experiment

Figure 1 shows the experimental room excavated in the granite rock mass. The place was selected in the unfractured zone in order to know the fundamental characteristics of the rock. An electric heater was positioned in a 66 mm  $\phi$  borehole drilled to a depth of 7 m from the wall of the drift. Arrangement of thermo-couples and thermal flux gauges around the heater is illustrated in Fig. 2. Electric power output for the heater has been adjusted from 1.7 KW to 2.4 KW in order to represent the power levels of the high-level wastes and kept constant for certain experimental terms.

Temperature changes were monitored in the granite rock adjacent to the heater. Fig. 3 shows an example of temperature changes at various radial distances which have been measured at 1.7 KW heating experiment as a function of heating time during 550 hours. Temperature isotherms around the heater at heating time of 600, 1114 and 1144 hours are shown in Fig. 4. The temperature increase curve as a function of heating time agrees with that of a prediction based on the heat conduction. Round symmetrical isotherms in all directions away from the axis of the heater also shows that the heat was transferred by conduction.

#### 4. Fracture Hydrology

Determining the permeability of the rock is an essential problem of understanding the groundwater movement. The Lugeon tests were attempted to measure the hydrolic conductivity of the granite.

In order to find the thermomechanical effect on permeability at the vicinity of the heater in unfractured zone, the Lugeon Tests were performed three times in connection with the rock heating. The permeability of the rock remained at a level below detectable limit, even at elevated temperature condition. Observations inside the hole using a borehole TV showed no serious fracture opening either. In order to measure the typical distribution of permeability in the rock mass around the experimental site and also to measure the water flow in the fractured zone, ( these tests are planned for next year ), the permeabilities were measured preliminary along the 46 m length borehole that was holed horizontally at 5 m above the experimental room. The results are shown in Fig. 5.

The rate of discharged water into the experimental room from the surrounding rock have been measured for 5.5 months. The results show a good correlation between the volume of seepaged water and a rainfall. These data are used for a validation of a computer code " 3D-SEEP " as described in the other chapter titled " Numerical model of groundwater flow ".

#### Reference

- 1) K. Shimooka et al., "Pilot Research Projects for Underground Disposal of Radioactive Waste in Japan", Radioactive Waste Management Vol.3, IAEA, (1984) 339.

Table 1 Characteristics of the from the test site

Density	2.64 g/cm <sup>3</sup>
Specific heat	0.18 (at 20 °C)
Thermal conductivity	$9.18 \times 10^{-1}$ cal/m·s·°C (at 20 °C)
Coefficient of thermal expansion	$3.8 \times 10^{-6}$ /°C (at 100 °C)
Poisson's ratio	0.19
Young's modulus	$5.5 \times 10^5$ kgf/cm <sup>2</sup>

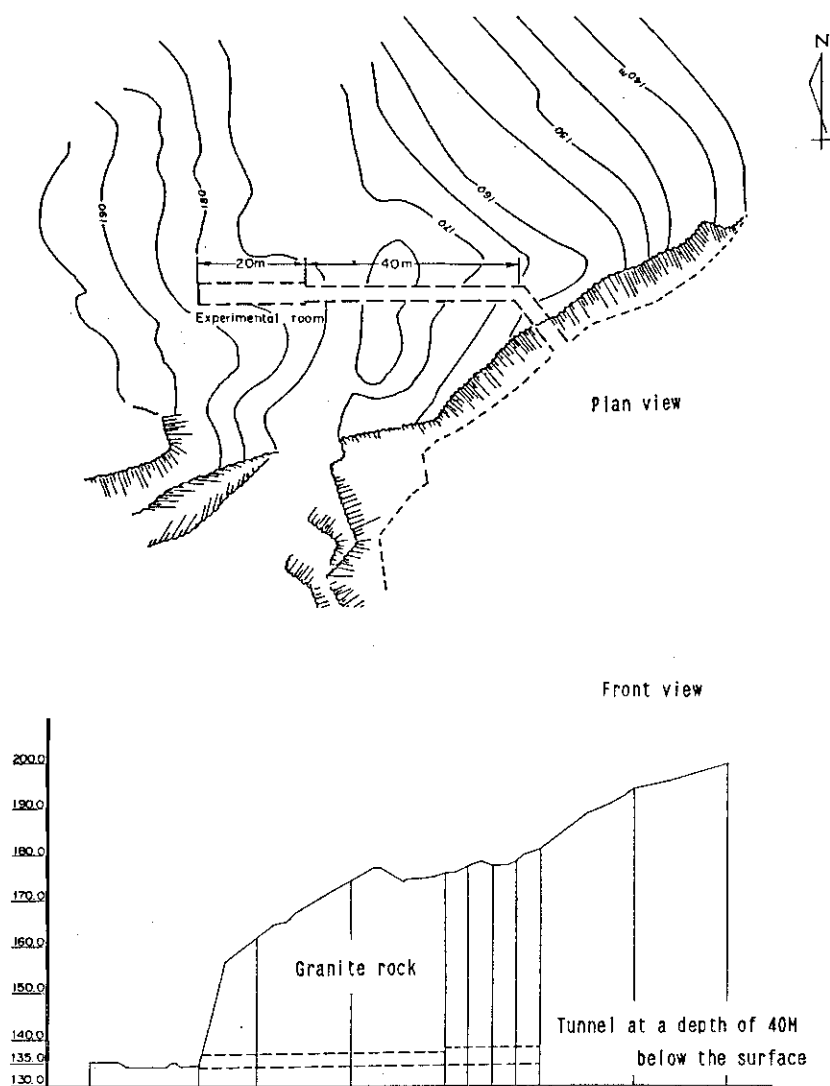


Fig.1 Location of experimental room excavated in granite rock



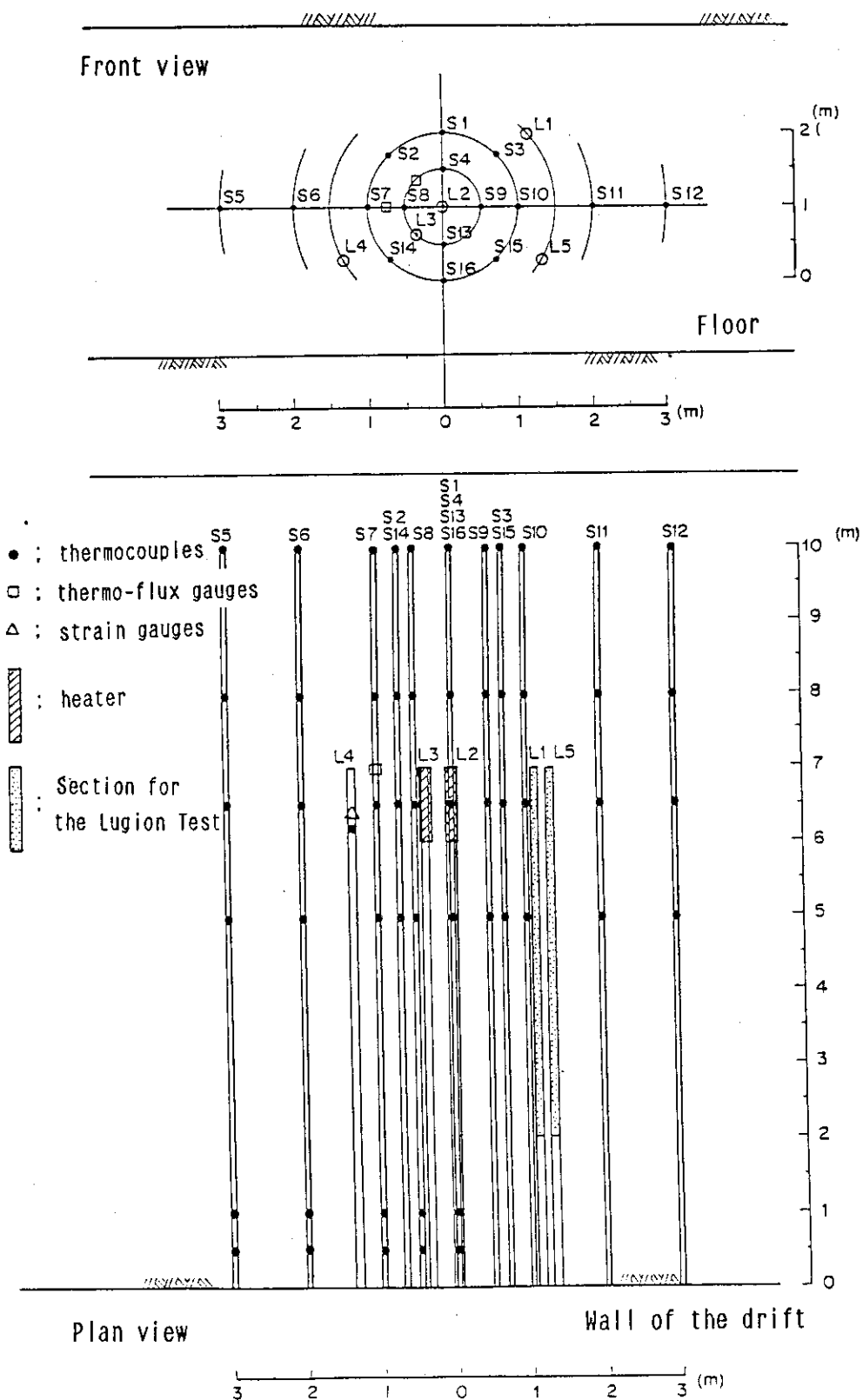


Fig.2 Arrangement of thermocouples, thermo-flux gauges and strain gauges around heater

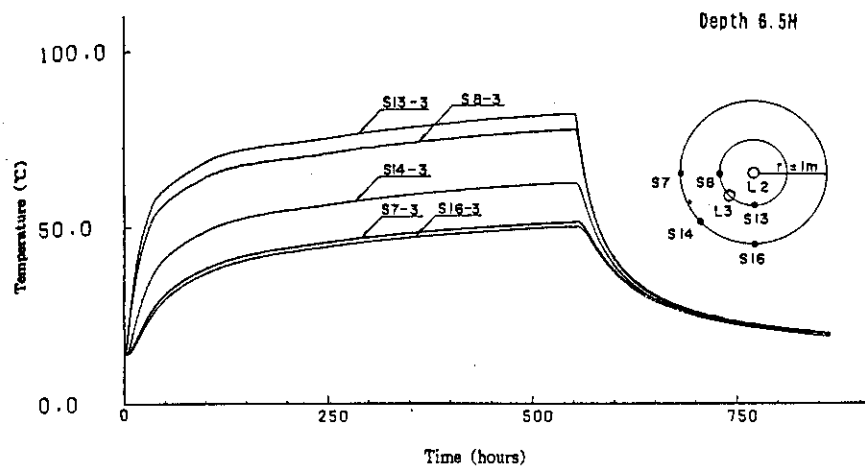


Fig.3 Temperature change at various radial distances  
as a function of time due to a constant out put (1.7KW)

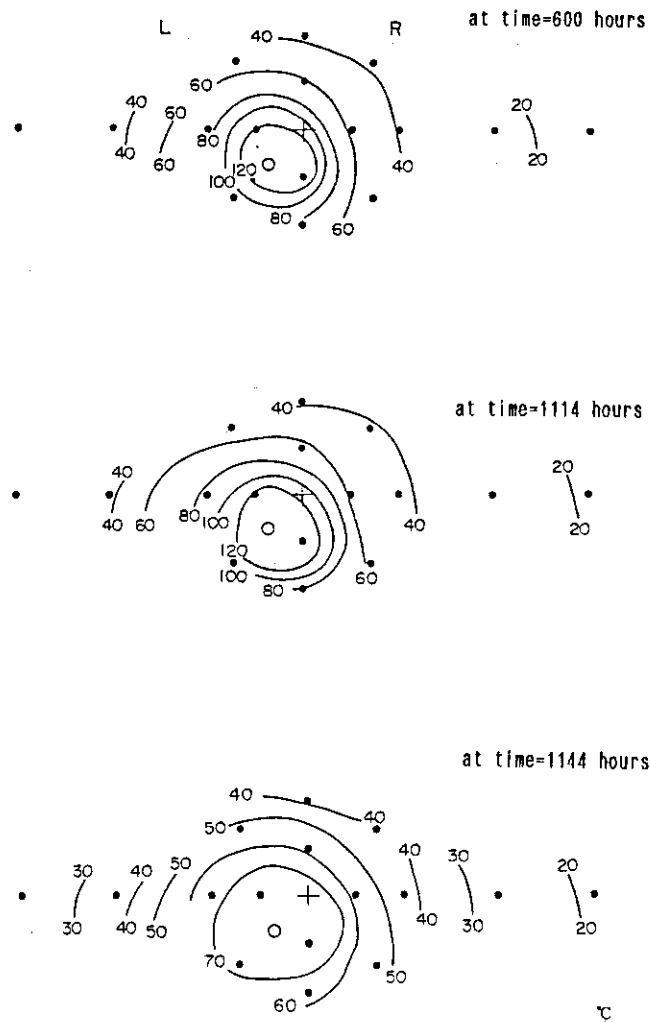
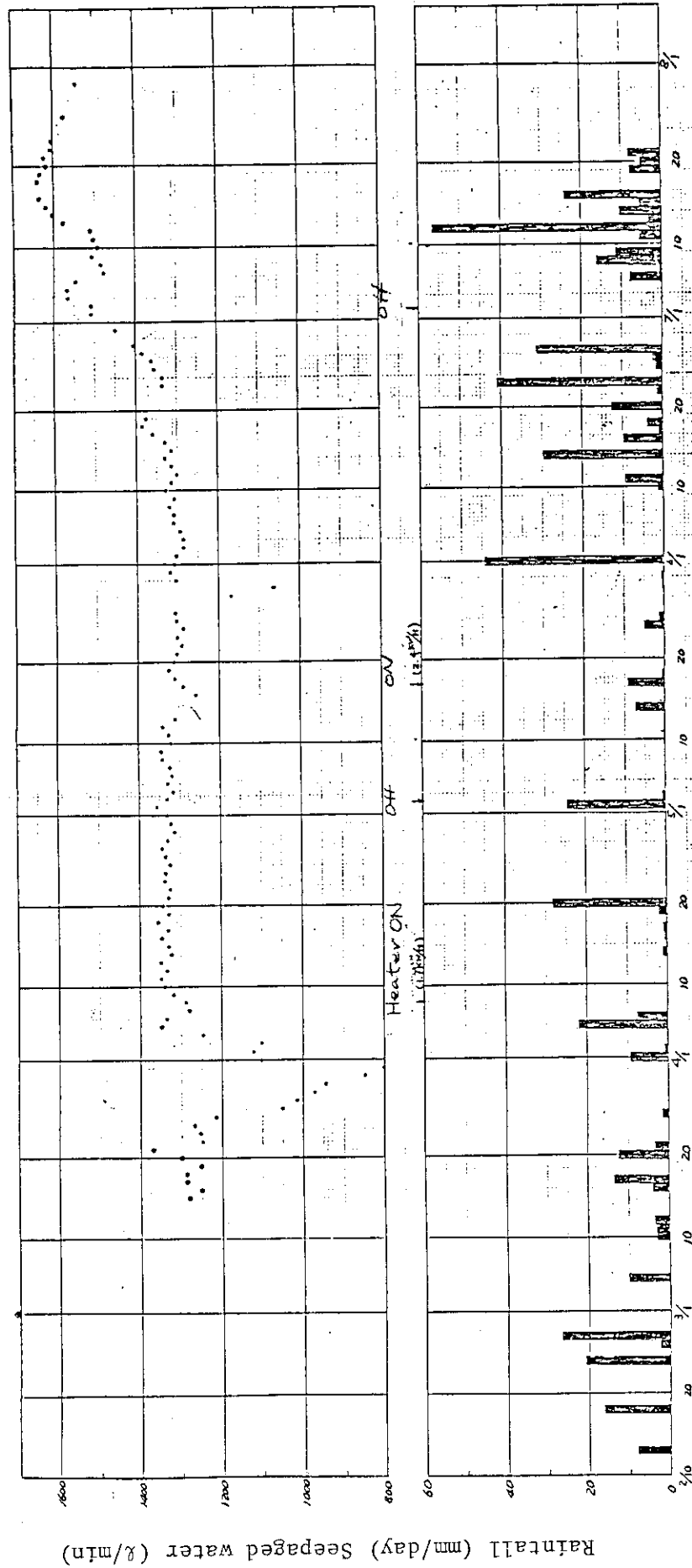


Fig.4 Vertical isotherms of temperature around the heater  
at time=600,1114and1144 hours



Measured date

Fig. 5 Correlation between rainfall and seepaged water into the room

## 2.5 In-situ Corrosion Test

A. Nakagoshi

### Introduction

Austenitic SUS, nickel base alloys and other alloys are recommended as candidate materials for a canister and a overpack case for high level radioactive waste (HLW). A corrosion resistance of these materials is one of the most important factors on the selection of alloys which will work as an artificial barrier in a disposal system. Stress corrosion cracking test (SCC) is carried out in-situ under two different temperature conditions in granite rock. These tests will be continued over two years.

### Experimental

The experimental conditions and the specifications of samples are listed in Table 1. The stress of the test materials has been applied by bending two coupon specimens into double U-bend type. All specimens are hanged to the frame with SUS-wires, and set in the two  $66\text{mm}\phi$  boreholes drilled in granite rock as shown in Fig. 1. and Fig. 2. Both holes (with and without heater) are filled with groundwater. In laboratory, the specimens of the same materials are set in deionized water at  $75^\circ\text{C}$ .

### Results

Results of 2 months later showed the properties of each material as follows.

In the in-situ test, all specimens with notches of SUS-304L and Hastelloy-C showed the stress corrosion cracking (SCC) in the case of high temperature condition ( $75^\circ\text{C}$ ). On the contrary, all plane type specimens showed no cracks and corrossions under the same condition. Under the normal temperature condition ( $20^\circ\text{C}$ ) all specimens showed no changes.

In the laboratory test, every SUS-304L specimens of both types showed SCC. Notched specimens of Hastelloy-C showed the cracks. Inconel-625 (notched type) showed the beginning of the cracking on the bending part of outer specimen.

Table 1 Specifications and Conditions of SCC

symbol	materials	Condition-1	Condition-2	Condition-3
A-P	SUS-304	3 pieces	3 pieces	3 pieces
B-P	SUS-304L	3	3	2
B-N	SUS-304L	3	3	3
C-P	SUS-304EL	1	1	1
C-N	SUS-304EL	3	2	2
D-P	Ticode	3	3	3
E-P	Inconel-825	3	3	3
E-N	Inconel-825	3	3	3
F-P	Inconel-600	3	3	3
F-N	Inconel-600	3	3	3
G-P	SUS-309S	3	3	3
H-P	Hastelloy-C	3	3	2
H-N	Hastelloy-C	3	3	2
I-P	Inconel-625	3	3	3
I-N	Inconel-625	3	3	3
T-P	Ti	3	3	3

P ; Plane Type

N ; Notched Type

Condition-1 ; In-situ at 75 °C (with heater)

Condition-2 ; In-situ at 20 °C (without heater)

Condition-3 ; Control experiment in labo. at 75 °C

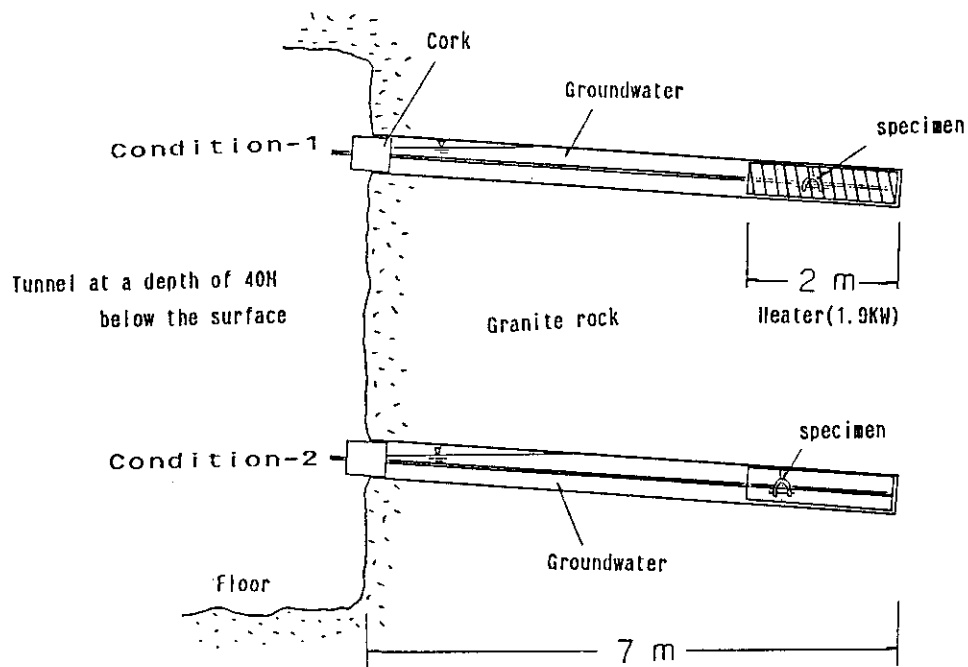


Fig. 1 Layout for in-situ corrosion test

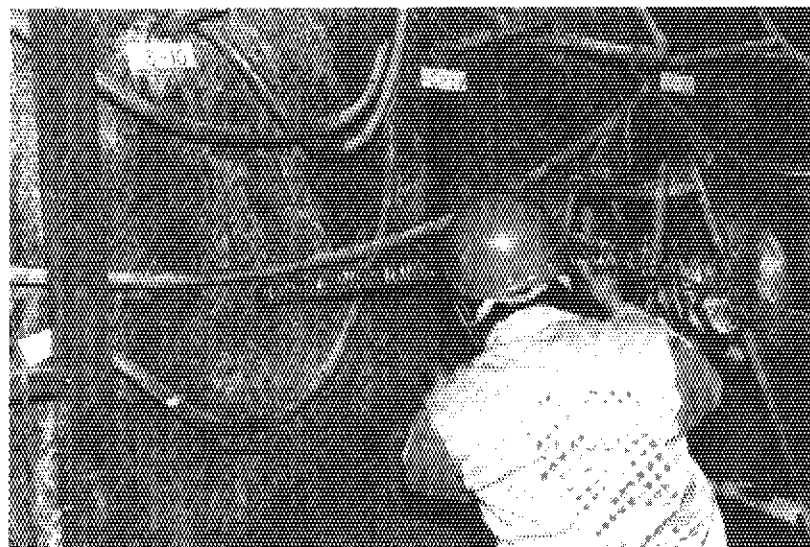
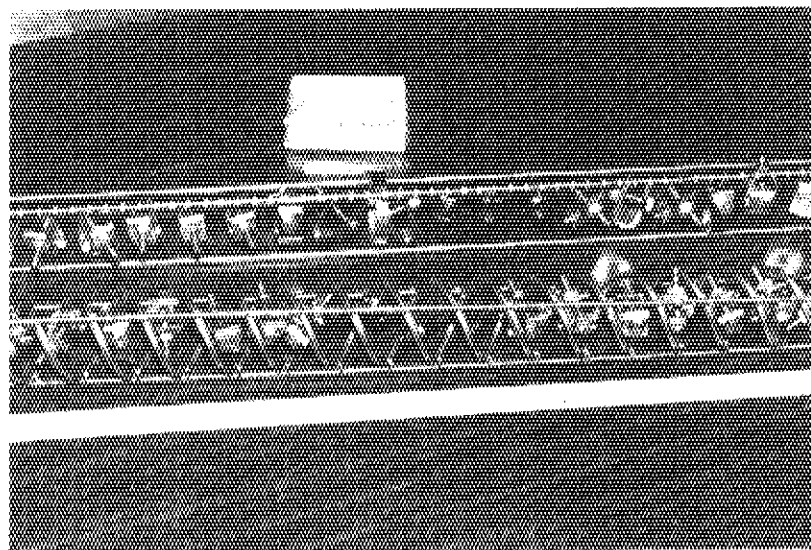


Fig. 2 IN-situ corrosion test

## 2.6 Accumulation of informations on characteristics of rock mass of deep underground from surveys for designing underground facilities

H. Nakamura

Data from underground facilities at granite site were collected last year. In this year, data were collected from geothermal survey and under sea tunnel construction.

### 1. Data from geothermal survey for geothermal power generation.

#### a) Distribution of temperature

The typical temperature distributions are shown in Fig. 1. Type 1 shows the temperature gradient at geothermal area, which is larger than usual geothermal gradient,  $10\text{ }^{\circ}\text{C} / 100\text{ m}$ . This value may be used to estimate the of near surface over the disposal site. Type 2 shows the distribution of the temperature in the case having impermeable layer. Type 3 shows hot aquifer layer. These large temperature gradients give some informations about the maximum gradient near repository in cases having fracture zones.

#### b) Temperature recovery after boring

Time dependence of the temperature distribution after boring are shown in Fig. 2. These data may be used to estimate the heat transfer by water flow.

#### c) Hydrothermal mineralogy

In order to estimate history of the temperature hydrothermal minerals have been used as an indicator. Elders and coworkers show the mineral zonation as shown in Fig. 3. These data are considered to be useful information of mechanisms healing fractures near repository and mineralization of nuclides leached from vitrified waste after very long term.

### 2. Data from tunnel construction under sea

#### a) Composition of fossil sea water

Composition of underground water have been used to know the origin of the water in coal mine under deep sea about 700 m from bottom. It has been known experiently that relative concentrations of Ca, Mg and  $\text{SO}_4$  are in special range for each origins: sea water, fossil sea water and ground water from land as shown in Fig. 4. This composition map may change site by site. However the composition of fossil water are

liable to offer usefull information to estimate long term reaction between grownd water and rock mass if it were related with geological age.

b) Composition of seepage water into SEIKAN tunnel

Seki and coworkers reported that the seepage waters were characterized according to whether they were well, moderately, or slightly interact. The elements showed different tendencies: K and Mg drop extensively and rapidly; Na drops moderately and slowly; Ca increases along with  $\text{SO}_4$ ;  $\text{HCO}_3$  drops. Close relationship between discharge rate and K content of the seepage waters is shown in Fig. 5. This information is considered to be useful to know the reaction rate between nuclides and rock.

Regarding all items serveyed in this year, we could not clear conclusion as safety assessment data bases, but we had pick up candidate items, which should be investigated in near future.

- 1) Elders, W.A. et al. "Hydrothermal alteration as an indicator of temperature and flow regime in the cerro prieto geothermal field of Baja California", Trans, Geothermal Resources Council, 4, 121 (1980)
- 2) Seki, Y. et al. : "The interaction between Miocene Volcanogenic Rocks and Sea Water-Meteoric Water Mixtures in Near Coast Undersea Part of the Seikan Tunnel, Japan



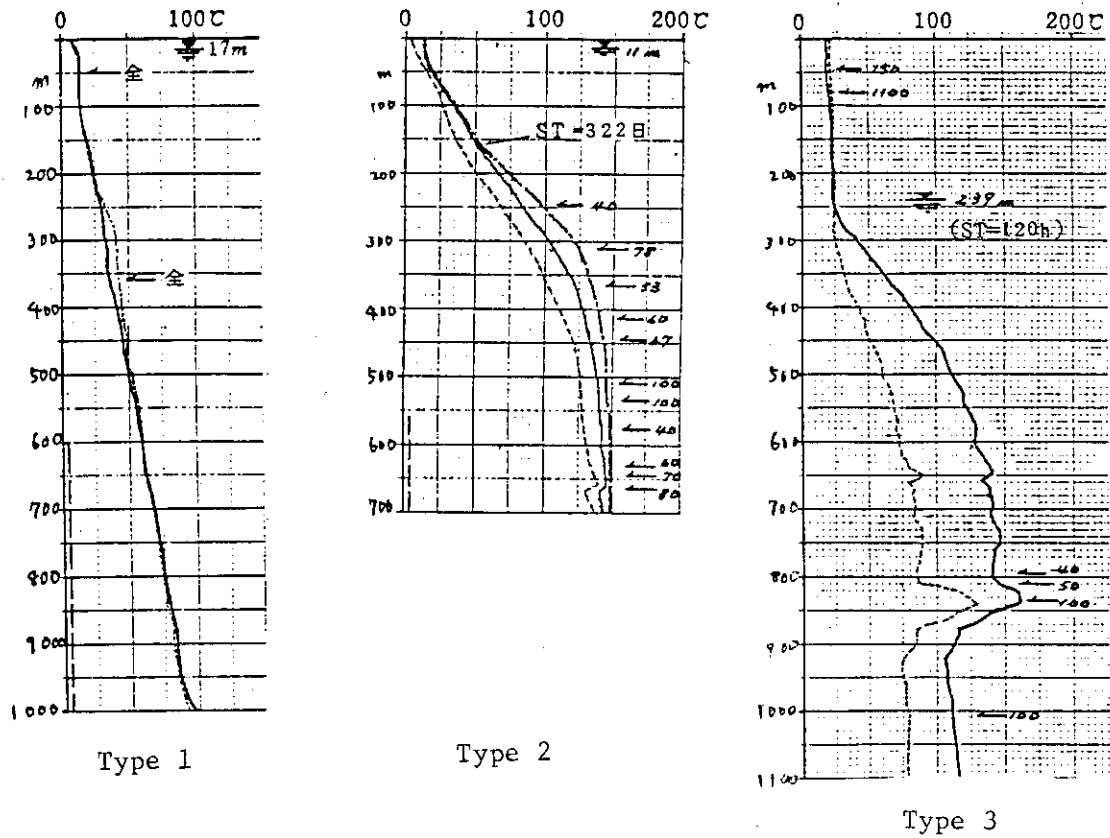


Fig. 1 Temperature distribution in geothermal area

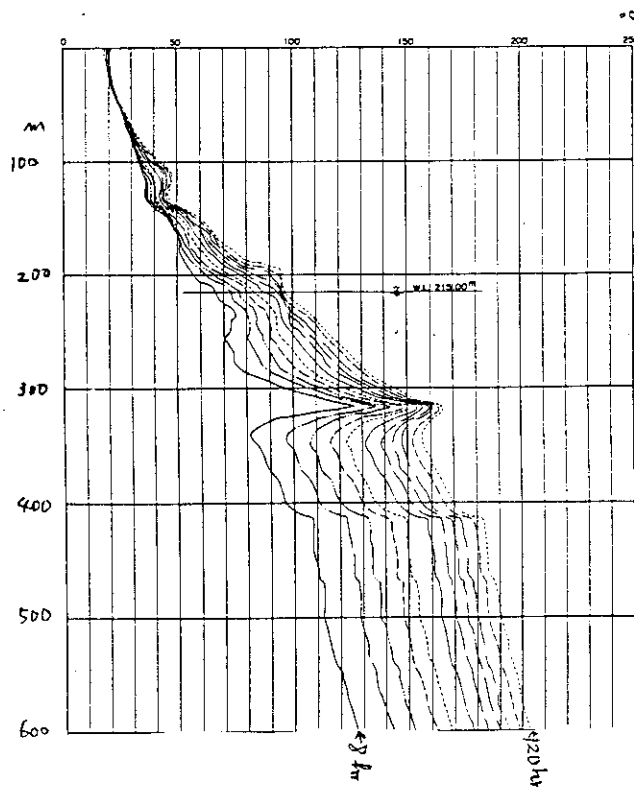


Fig. 2 Temperature distribution after boring

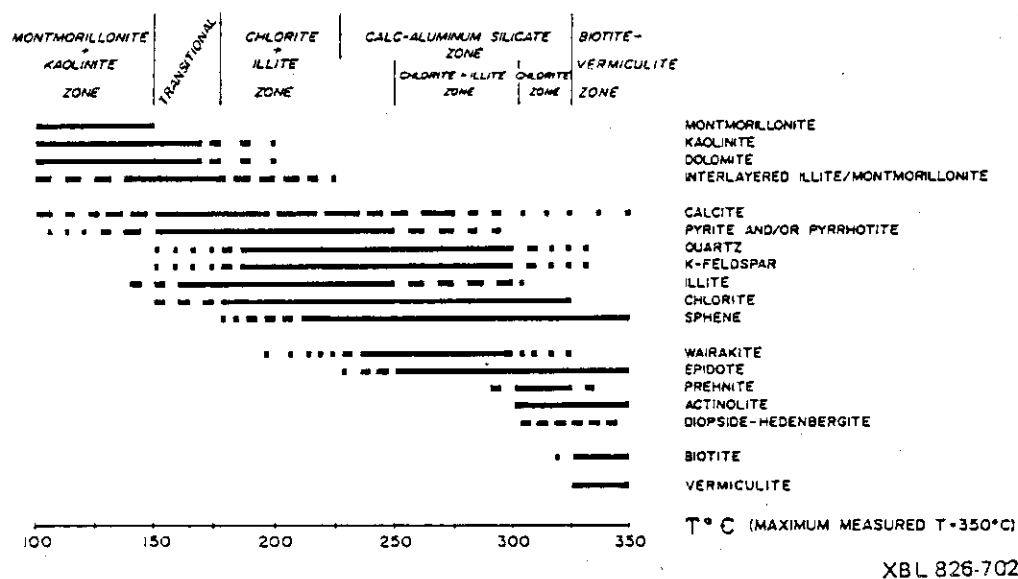


Fig. 3 Temperature ranges of mineral zones in sandstones from the subsurface at Cerro Prieto (modified from Elders et al., 1979)

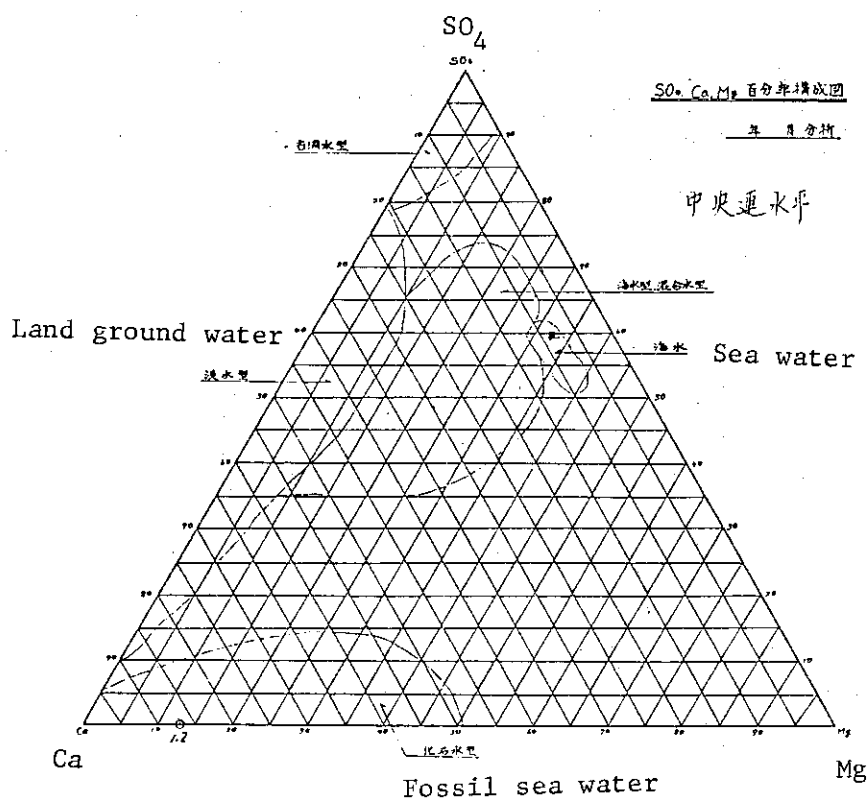


Fig. 4 Composition of ground water from various origin

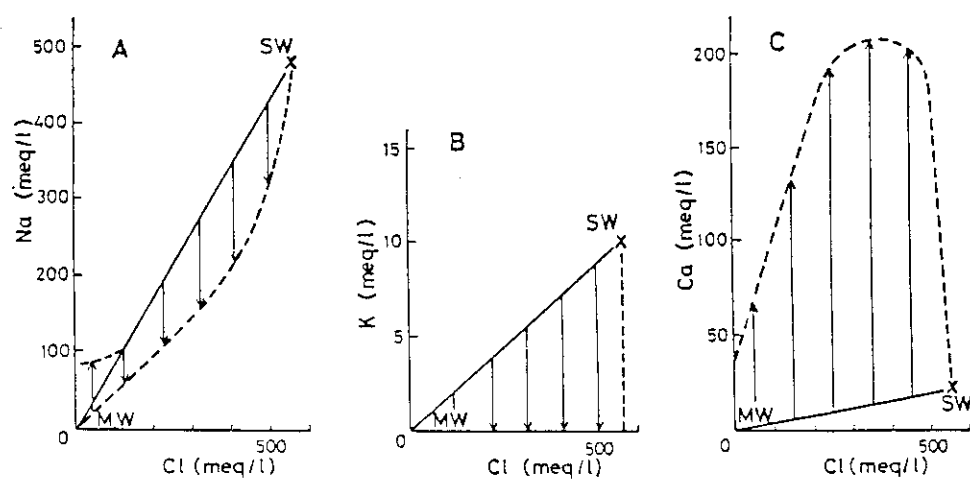


Fig. 5 Na, K, Ca -versus- Cl diagram for seepage waters of the Seikan Tunnel

## 2.7 Numerical model of ground water flow

H. Kimura

### Introduction

The joint research program concerning radioactive waste of JAERI and U.S.NRC was started in 1984. JAERI proposed the intercomparison study with JAERI's code and NRC's code about the analysis of ground water flow at the JAERI's experimental site. It is planned that NRC uses SWIFT and TOUGH code, and JAERI uses 3D-SEEP code in this study.

An international study for comparing hydrology models (HYDROCOIN) was started in May 1984 under management of the Swedish Nuclear Power Inspectorate (SKI). JAERI participates as one of the coordinating group. The study comprises, the impact on the ground water flow calculations of different solution algorithms, the capabilities of different models to describe field measurements, and the impact on the ground water flow calculations of incorporating various physical phenomena. It is planned to conduct the study on three successive levels. The primary objective of level 1 is to check the numerical accuracy of the codes, by intercomparison or by comparison with analytical solutions. Secondary objectives are the development of discretization strategies for achieving cost effective but accurate solutions, and to exchange ideas on pre- and post-processing techniques. Level 2 will deal with validation of codes against experimental data. Level 3 will consist of sensitivity and uncertainty analyses.

The option of transient calculation is added to the computer code 3D-SEEP to perform the level 1 study in JAERI. Crank-Nicholson method

is adapted for the discretization of time, and the linearity of the equation is assumed at each time step.

#### The study of joint research with U.S.NRC

The problem of this study is the simulation of steady state flow in a three dimensional domain representing a test site of granite rock. The domain is shown in Fig.1. The hydrologic system consists of two material layers : a high hydraulic conductivity layer of weathered granite overlays on a layer of granite. The layer of weathered granite is unsaturated media, and the hydraulic property of weathered granite is shown in Fig.2. It is assumed that the hydraulic conductivities of weathered granite and granite have isotropic and homogeneous properties.

Although the tunnel and fracture exist as shown in Fig.1, we neglect the size of tunnel and the fracture in the preliminary calculation. The effect of tunnel is only taken into account by restricting the pressure head of tunnel floor to be zero. The calculated pressure head at the point of 5m below the tunnel floor is 9.7m, and this is slightly larger than the experimental value of about 9.0m. The reason of this difference may be mainly due to the underestimate of leakage-water from the tunnel. The calculated pressure head contours in the Y-Z plane at X=60 m are shown in Fig.3. A dot line of this figure means water table. Further calculations including the tunnel and fracture are now in progress.

#### HYDROCOIN study

For level 1 the following seven cases were originally proposed.

- Case 1 ; Comparison of numerical solutions with an analytical solution to a problem involving transient flow from a bore hole in a permeable medium containing a single fracture.
- Case 2 ; Simulation of steady state flow in a two dimensional domain containing two permeable fracture zones. The zones are inclined so that they intersect at a certain depth.
- Case 3 ; Simulation of partially saturated flow through a sequence of alternating pervious and low permeability sedimentary rocks.
- Case 4 ; Comparison of analytical and numerical solutions of thermal convection driven flow. The heat is evolved from a spherical source with a decaying heat output. The thermal bouyancy is the only driving force.
- Case 5 ; Simulation of water flow and salt transport in a two dimensional domain. The fluid density is linearly dependent on the salt concentration.
- Case 6 ; Simulation of steady state flow in a three dimensional domain representing a generic bedded salt situation. The domain is shown in Fig.4.
- Case 7 ; Simulation of steady state flow through a shallow land burial site in argillaceous media. The calculations involve saturated flow and the modeling of a seepage face.

We calculated the four cases ( case 1, 2, 6 and 7 ) of level 1 study using 3D-SEEP code, and got good agreements with the examples of initial attempt. Calculated result of case 6 is shown as a representative of level 1 study. Hydraulic head contours in vertical cross section along the southern boundary are shown in Fig.5 together with the result of SWENT code.

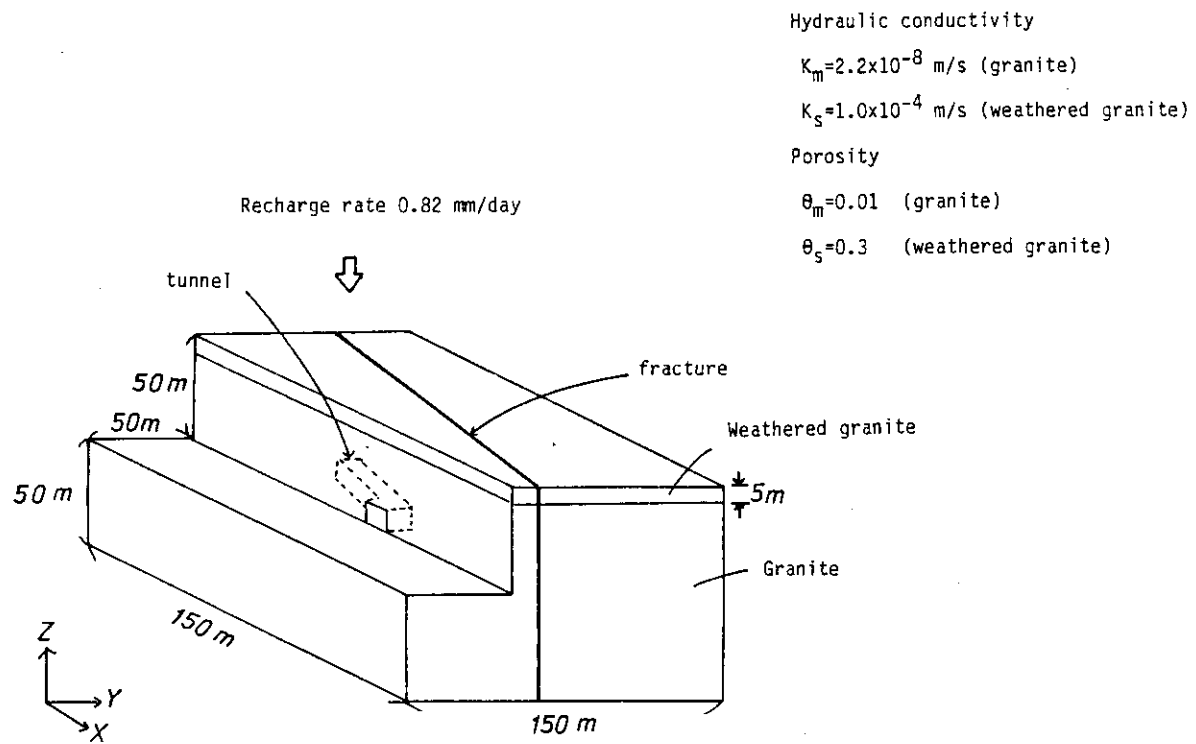


Fig.1 Modelled domain for the joint research

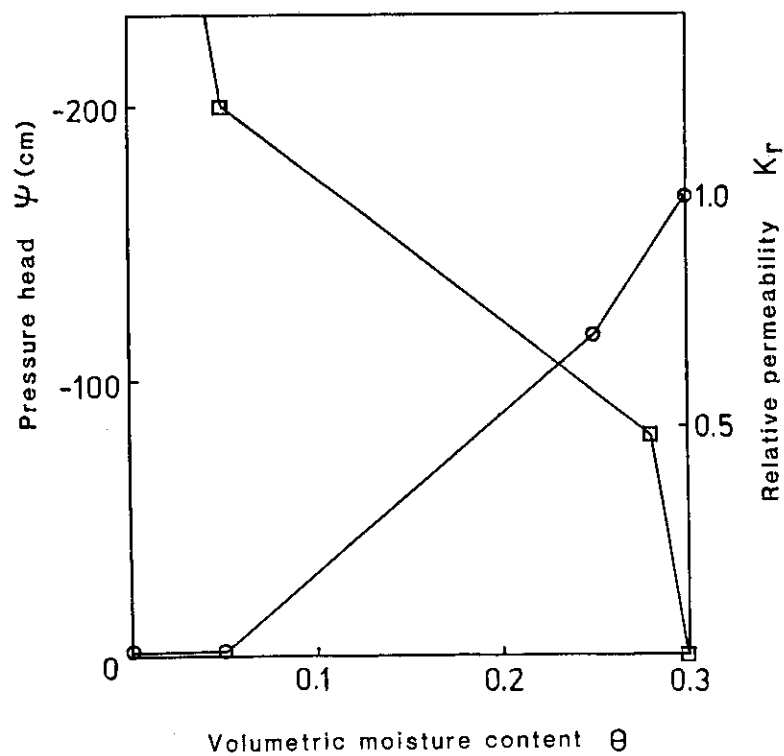


Fig.2 Hydraulic property of weathered granite





\*\*\* CASE 8-85.2.15 \*\*\*

\* TOTAL H CONTOUR FIG. OF SECTION X-Z \*  
SECTION Y = 0.000E+0

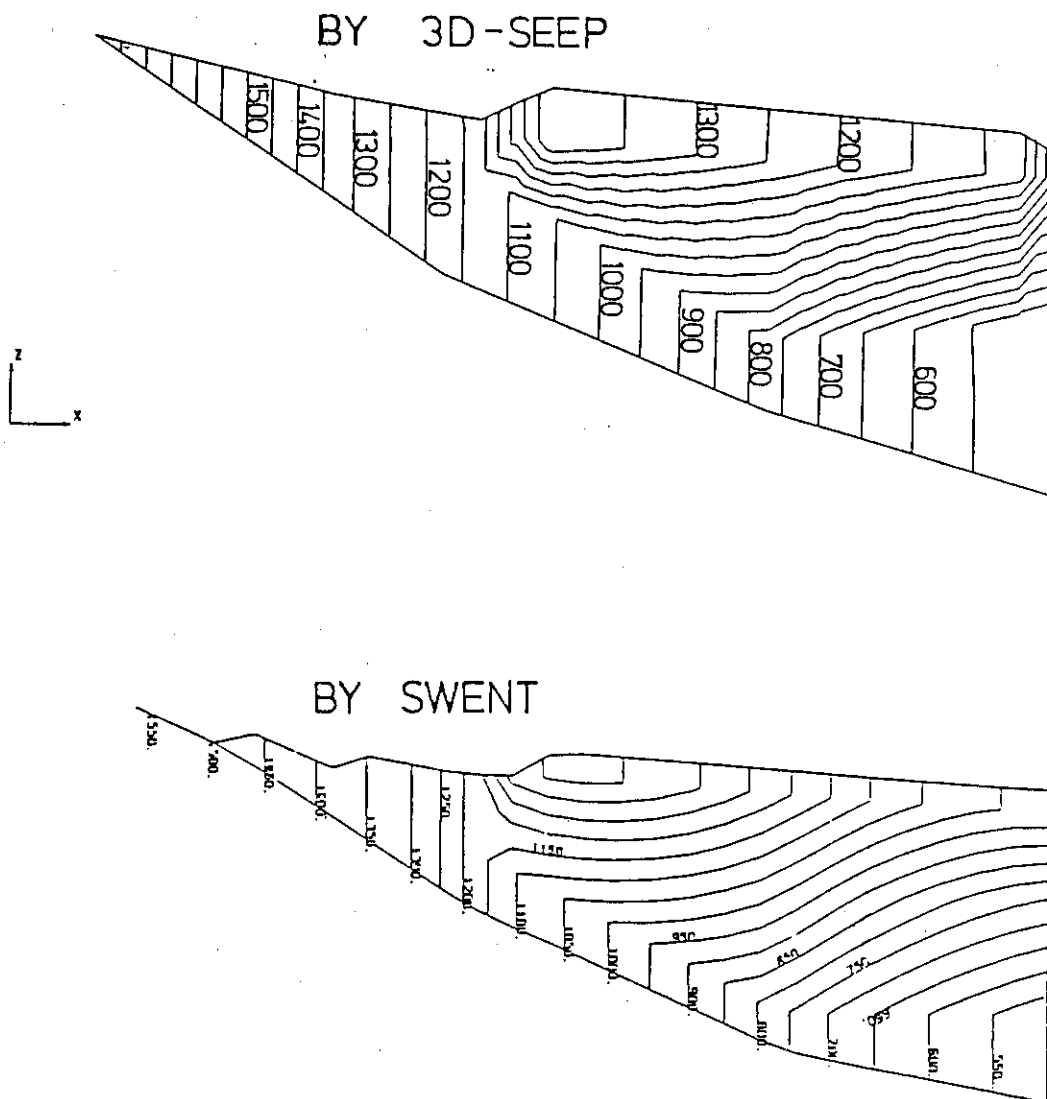


Fig.5 Total head contour in vertical cross section along the southern boundary

### 3. Safety examination of vitrified forms in the hot cells of WASTE F

S.Tashiro

The Waste Safety Testing Facility (WASTE F) has performed hot operations since November, 1982 in order to obtain data on the performance and durability of materials for the long-term isolation of high level radioactive wastes.

In this fiscal year, studies on leachability of plutonium, leaching test of real waste product on a co-operative program with PNC, improvement of autoradiographic techniques for the identification of alpha nuclides in glass samples and safety assessment study of proposed specifications of to-be-returned wastes from COGEMA and BNFL using results from WASTE F tests have been carried out besides the following briefly described items.

### 3.1 Production of radioactive vitrified test samples

J.Morita

Four radioactive vitrified products have been prepared for safety tests in this current year including two ones made with vitrification apparatus in Fig. 1. Table 1 gives an outline of these runs with the apparatus. Each sample was made with synthetic wastes contained radioisotopes, which were fed directly into the melter of apparatus and treated in a sequence of processes of calcination, melting, mixing, conditioning and off-gas treatment. Temperature of calcination and melting were 750 °C and 1200 °C respectively, and each operating time was about 3 hrs. The mixing operation was continued for thirty minutes with bubble of air that was carried through a pipe(11 mm ID) at the rate of 20 cc/sec.

Fig. 2 shows a new fiber scope attached under the melter to observe molten glass falling into the receiver. Also the scope can be removed out from a setting unit with remote operation and used for observing conditions of outer parts of the vitrification apparatus. When the molten glass having comparatively high viscosity pass through a fine tube of the melter and reach to canister, it would take a longer time to the end of falling the glass. In such cases, the molten glass would be misled to the outside of canister. This scope is useful to find out such kind of troubles.

Table 1 Specification of vitrification

Run No.	Composition of product			Weight of product (g)	Purpose of production
	Matrix	Waste (Content, wt%)	RI (Activity, mCi)		
H84001	*	JW-C (23.1)	Cs-137 ( 90) Cs-144 ( 500)	1337.0	Radioactive homogeneity measurement
H84002	*	JW-C (23.1)	Cs-137 ( 230) Cs-144 (1560)	1311.0	Leachability examination

\* Each matrix was composed of  $\text{SiO}_2$  (45.2wt%),  $\text{B}_2\text{O}_3$  (13.9),  $\text{Na}_2\text{O}$  (6.1),  $\text{Al}_2\text{O}_3$  (4.9),  $\text{CaO}$  (4.0),  $\text{Li}_2\text{O}$  (2.0) and  $\text{ZnO}$  (2.5).

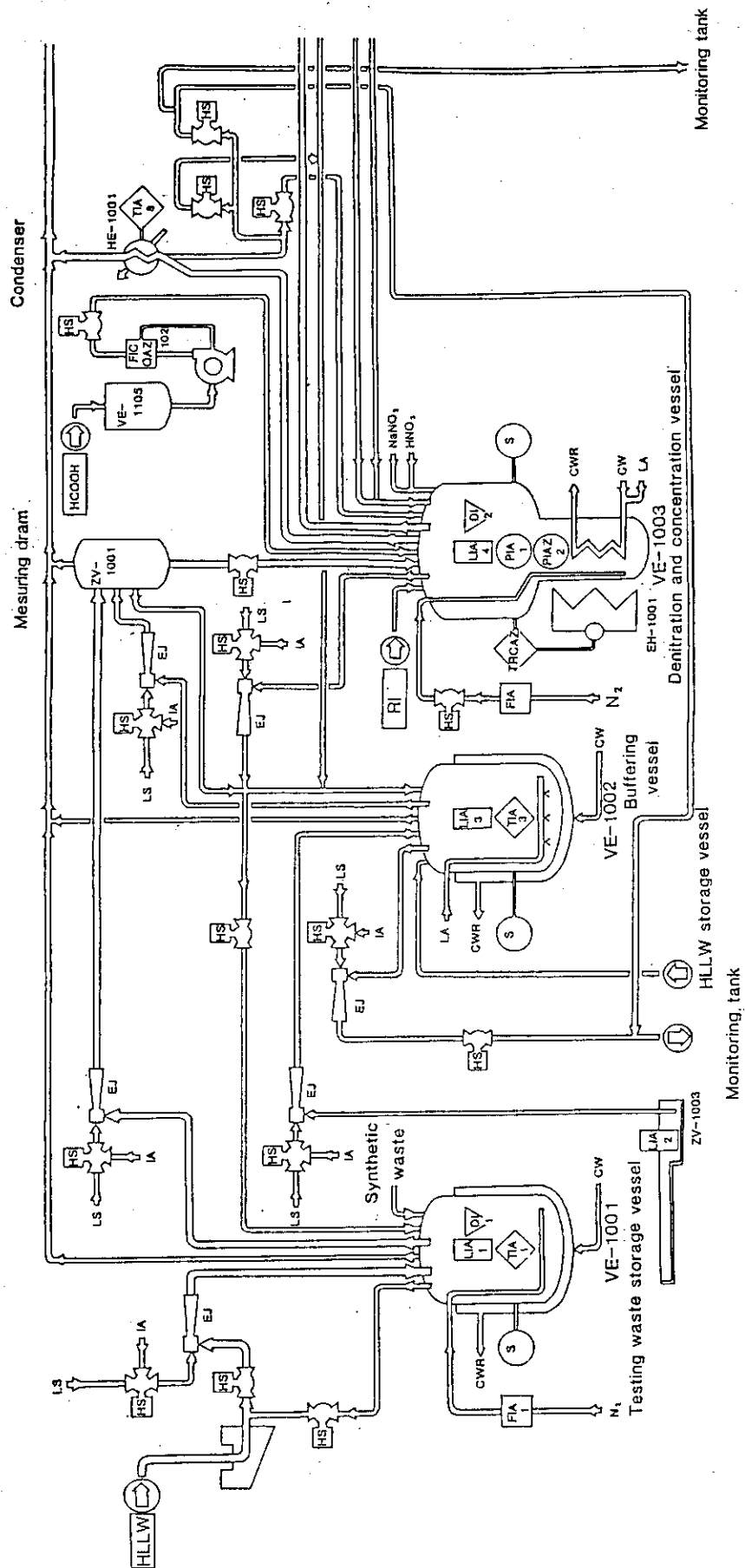


Fig. 1 Process flow of the vitrification apparatus (1)

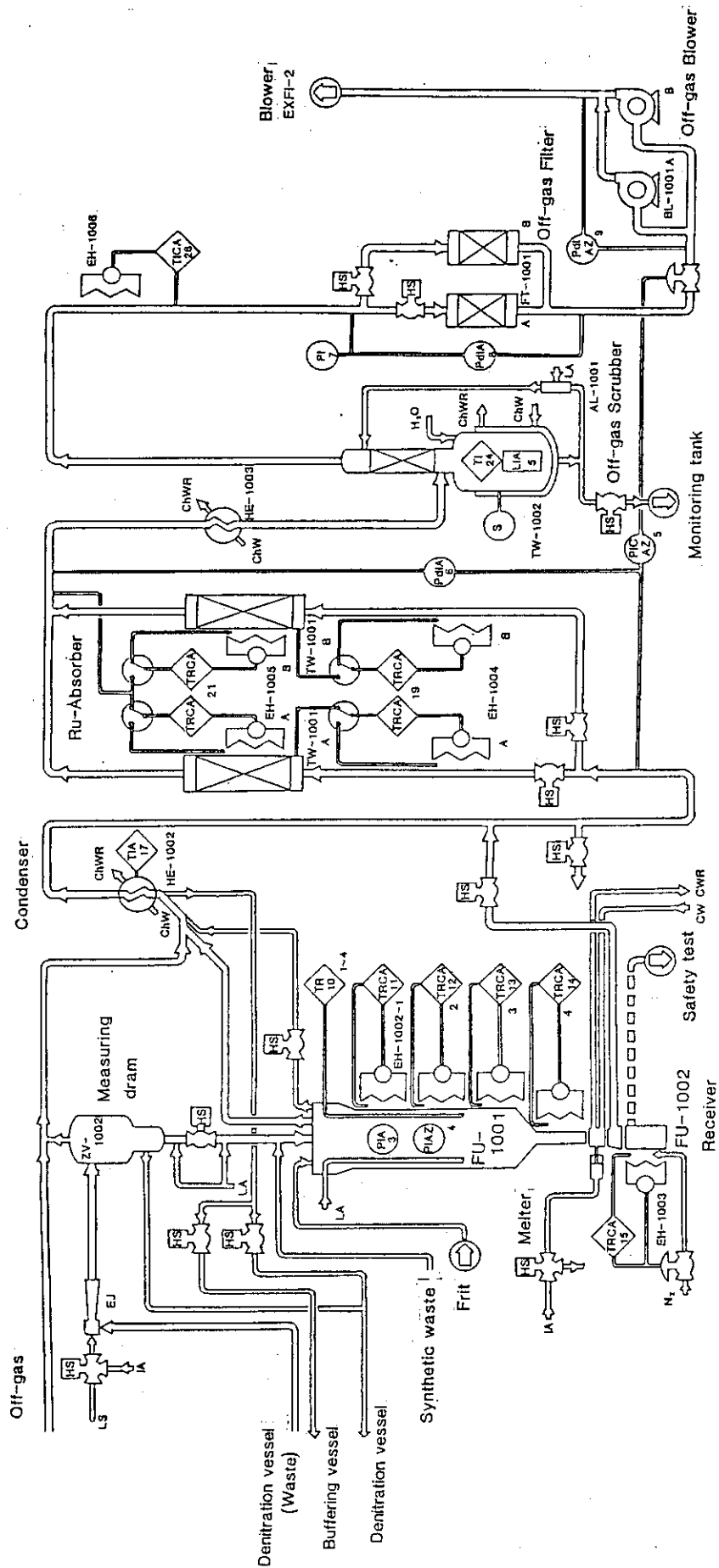


Fig. 1 Process flow of the vitrification apparatus (2)

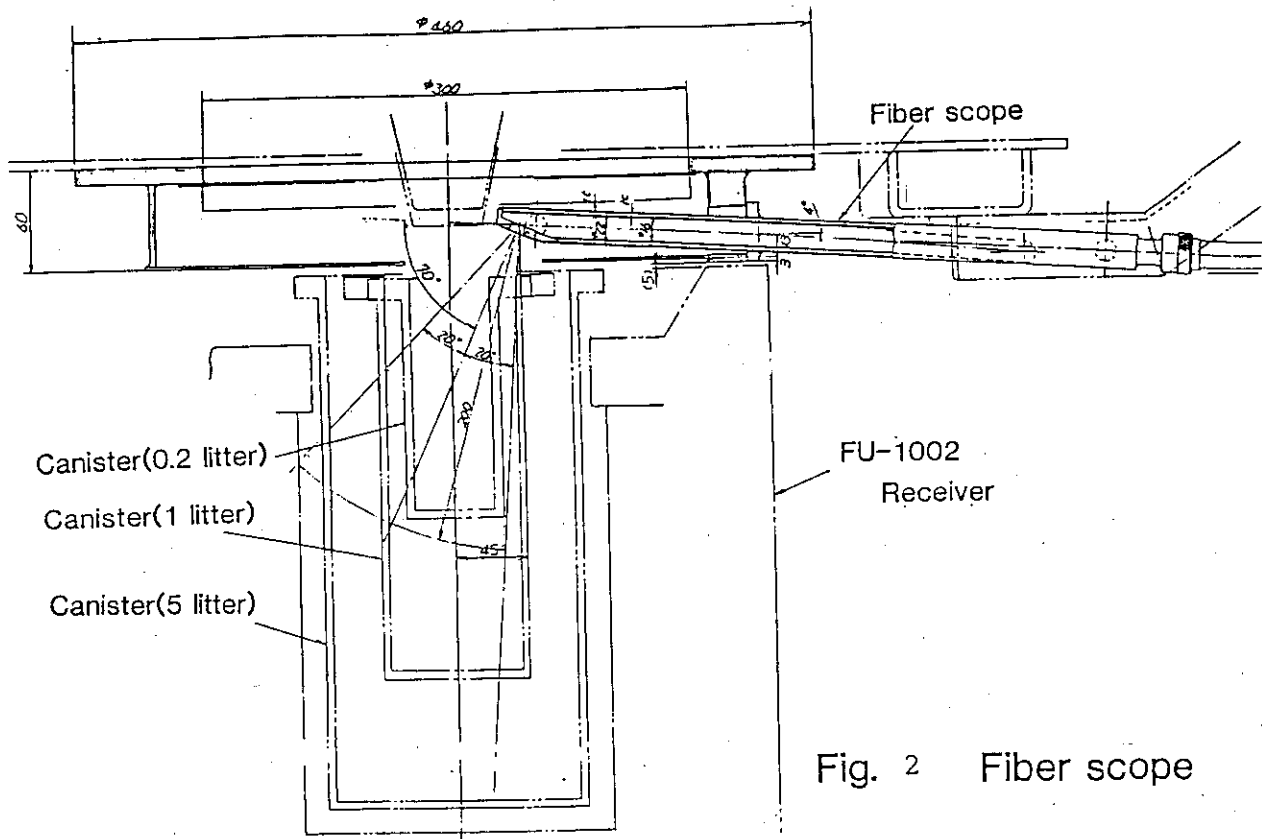


Fig. 2 Fiber scope

### 3.2 Development of a recycle system of cooling water containing glass slurry

S.Kikkawa and M.Nomura

The No.3 cell has the sample preparation apparatus such as cutter, core drill, polisher etc. for the purpose of making test specimen from vitrified blocks. Most of them need cooling water and make glass slurry into the water in operation. The increase of radiation dose near the drainage process by the glass slurry was one of the important factor to be taken into consideration for the easy maintenance of the cell. A system has been developed to improve maintenance and service ability of the cell by collecting and filtering glass slurry. Outline of the system flow is shown in Fig. 1.

The important points of the system design are as follows;

- (1) Quick collection of glass slurry was established by application of a cone shaped thickener and a wash-away device attached to the thickener using drainage water passed through filters.
- (2) Specification of filter elements was fixed to meet the size distribution of glass slurry generated from the apparatus ( Fig. 2).
- (3) Exchange of filter elements can be operated in remote manipulation.

The system performance was confirmed by the radiation measurement near the process to find background level after the cutting operation of 1 litter vitrified product contained about 200 mCi of Cs-137, while the radiation dose rate was about 150 mR/h at the surface of filters.



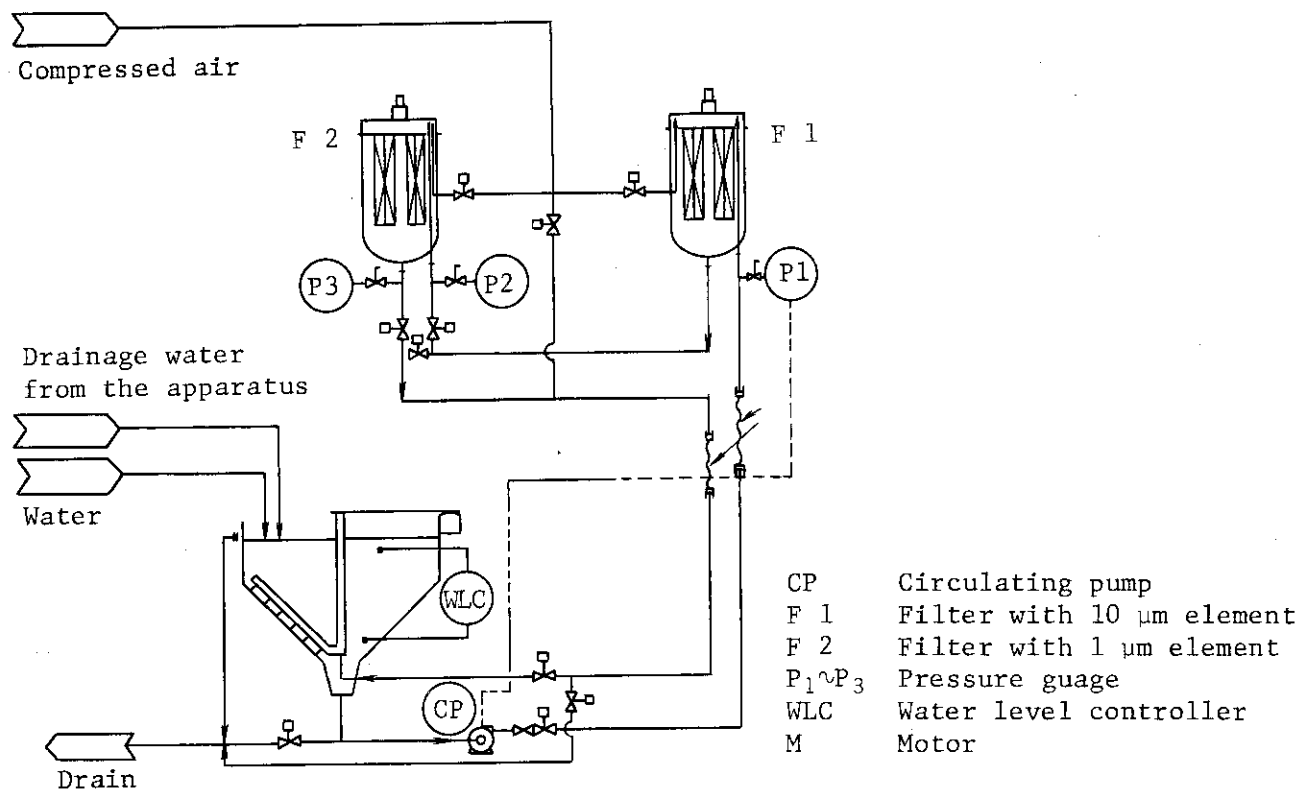


Fig. 1 Flow diagram of the system

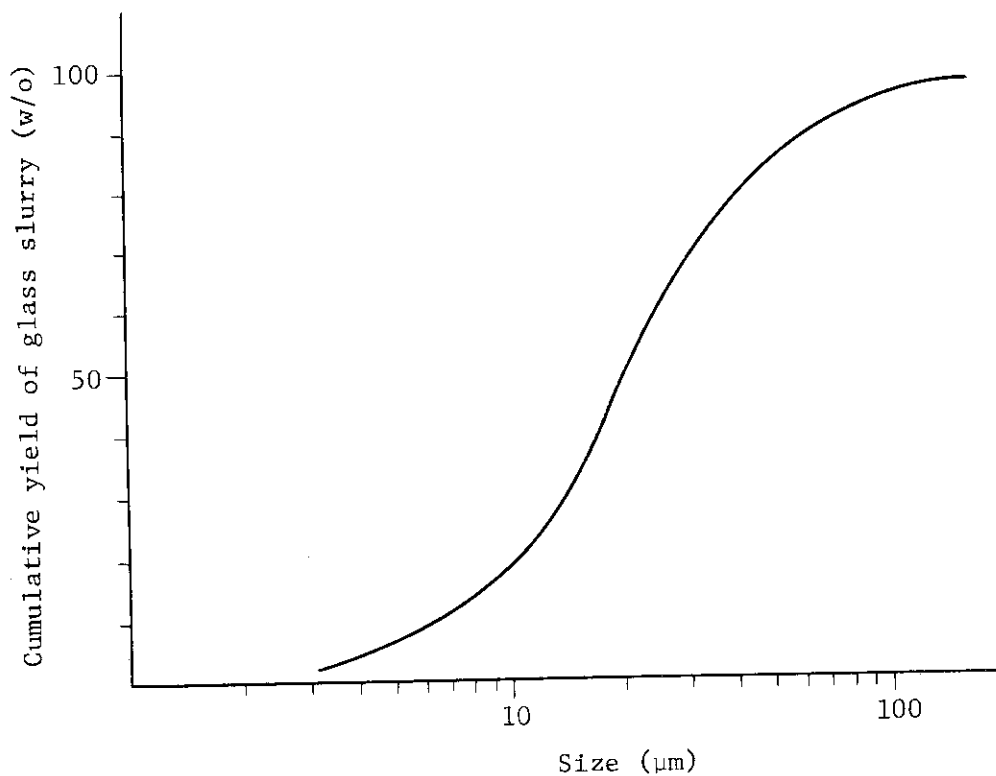


Fig. 2 Size distribution of glass slurry

### 3.3 Preliminary experiments on contamination of metallic surfaces caused by HLW glass

O.Kuriyama

When molten glass containing high level waste (HLW) is poured into a canister, the surface of canister will be contaminated by spill of glass itself and radioactive vapor from the glass. The contamination might cause a kind of air contamination at special conditions of storage duration of glass. Preliminary experiments on fundamentals of the waste glass adhesion to metals have carried out to get some information for assessing the safety of storage facility.

The molten waste glass was dropped at 1150°C on metal specimen as shown in Fig.1 and the weights of dropped glass and adhered glass to metal specimen were measured. The adhesion factor is defined as the ratio of the adhered to the dropped weight.

The relationships between the initial surface temperature of the metal specimen and the adhesion factor were examined to clarify the adhesive behavior of the molten glass for some candidate materials. Figure 2 shows that the adhesion factors of stainless steels (SUS 304L, SUS 309S) and inconel (INCONEL 600) increased with the initial surface temperature at initial contact with the molten glass above 450°C. On the other hand, the adhesion factors of titanium were approximate zero below 650°C. Besides, neither cesium nor strontium on the titanium could be detected by means of flame atomic absorption spectroscopy and inductively coupled plasma atomic emission spectroscopy. Hence

other adhesion experiments are being planned using radioactive waste forms in 1985. This experiments will aid in determining very low levels of contaminations on the specimens of approximate zero adhesion factor.

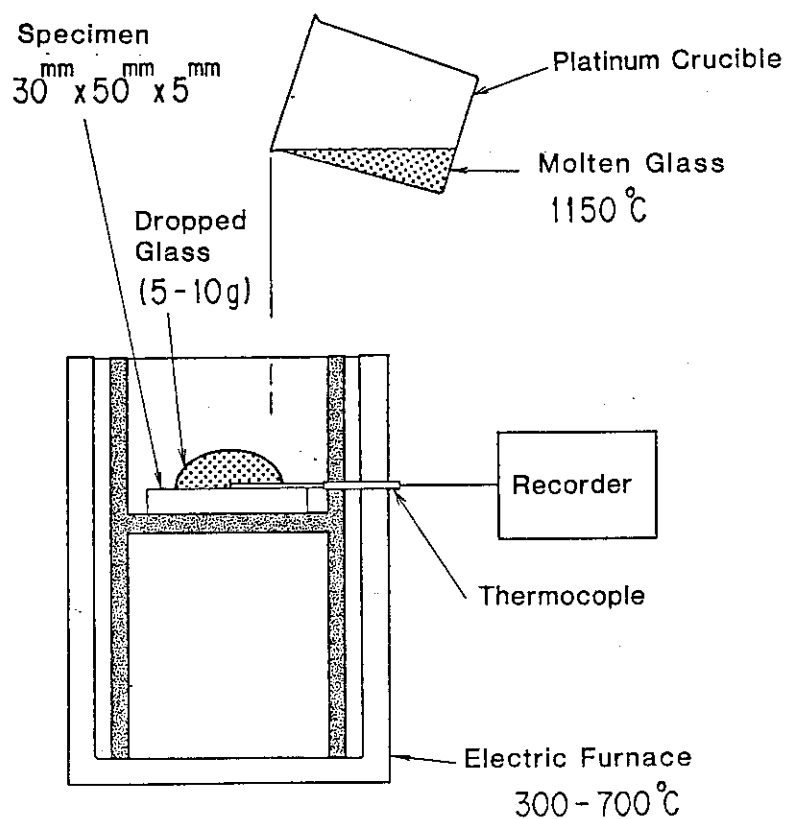


Fig.1 Concept of equipment

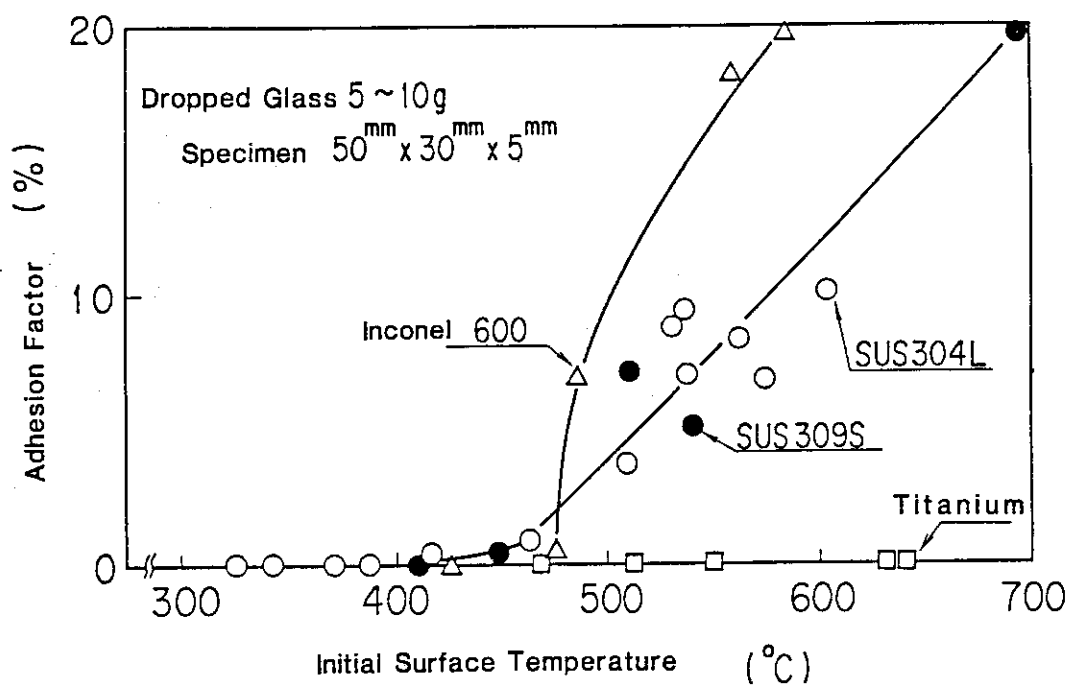


Fig.2 Adhesion of molten HLW glass to some metallic surfaces

### 3.4 VOLATILIZATION OF CESIUM FROM NUCLEAR WASTE GLASS IN A CANISTER

Hiroshi Kamizono

In this work, the volatilization of Cs-134 from simulated high-level waste glass in a one liter-canister in a temperature range from 25°C to 1000°C was examined. The glass was poured into the canister in order to more closely approximate a realistic situation. Cs-134 was selected for research purposes because it is more easily handled than Cs-137 due to the shorter half-life of Cs-134. The results obtained showed that the amount of Cs-134 suspended in the air inside the canister was significant even at waste storage temperatures below 500°C when the glass had been subjected to several reheatings up to a maximum of 1000°C.

#### EXPERIMENTAL

Simulated high-level waste glass used for this study was borosilicate glass containing about 12.7 wt% of simulated fission products and actinides. The reagents for the glass additives and the simulated high-level waste were mixed simultaneously and placed in a vitrification apparatus<sup>[1]</sup> with a solution of 0.51 Ci of Cs-134. This mixture was calcined at about 750°C, melted at 1200°C for 2 hours, poured into a stainless steel canister (8.1 cm in inner diameter and 24.4 cm high) and then cooled to room temperature.

The total amount of Cs-134 in the simulated high-level waste glass was measured by a gamma-scanning method<sup>[2]</sup>.

The glass, containing Cs-134, in the canister was heated in a

electric furnace (Fig.1) at given temperatures in a range of 25°C to 1000°C for up to 4 days. The schematic heating conditions are shown in Fig.2. The glass was heated from 25°C to five given temperatures, i.e., 1000°C, 900°C, 900°C, 700°C and 400°C in this order. The temperature was measured near a middle point in the air inside the canister because it was almost equal to the temperature in the middle of the glass. During the course of heating (see solid lines in Fig.2), part of the air in the upper space of the canister was collected in a sampling bottle (about 7.5 cm<sup>3</sup> in volume) via a sampling needle (about 50 cm in length and 0.9 mm in inner diameter) (Fig.1), both of which were made of stainless steel. The sampling bottle was vacuumized before use, and pierced by the sampling needle which was inserted into the canister.

## RESULTS AND DISCUSSION

### (1) AMOUNT OF CESIUM IN THE GLASS

The total amount of Cs-134 in the glass was measured to be about 0.44 Ci by the gamma-scanning method<sup>2</sup> using a standard radioactive control (Eu-152). The volume of the glass was estimated to be about 430 cm<sup>3</sup>.

### (2) TIME-DEPENDENCE OF VOLATILITY OF CESIUM

The time-dependence of the amount of Cs-134 in the air inside the canister at 600°C and 700°C is shown in Fig.3. The amount of Cs-134 in the air inside the canister ( $A_{\text{Cs-134}}(\text{Ci/cm}^3)$ ) was assumed to be expressed as,

$$A_{\text{Cs-134}} = (a \times R_{\text{Cs-134}}) / V_{\text{st}} \quad (1)$$

where  $a$  is the correction factor for the decay of Cs-134,  $R_{\text{Cs-134}}$  (Ci) is the radioactivity of Cs-134 trapped by both the sampling bottle and the sampling needle and  $V_{\text{st}}$  ( $\text{cm}^3$ ) is the volume of the vacuumized sampling bottle. The detection limit for measuring  $A_{\text{Cs-134}}$  was about  $1 \times 10^{-11}$  Ci/ $\text{cm}^3$ . Figure 3 shows that  $A_{\text{Cs-134}}$  reaches a constant value after a short soaking time of less than 2 hours at 600°C and 700°C.

### (3) TEMPERATURE-DEPENDENCE OF VOLATILITY OF CESIUM

Figure 4 shows the relationship between  $A_{\text{Cs-134}}$  and the inverse of the absolute temperature at a fixed soaking time of 1 day.  $A_{\text{Cs-134}}$  at 200°C and 400°C in the first cycle of reheating could not be measured because it was less than the detection limit. Figure 4 indicates that the temperature-dependence of  $A_{\text{Cs-134}}$  can be divided into two categories. For temperatures above 500°C,  $A_{\text{Cs-134}}$  increases with increasing temperature, and the vaporization heat was calculated from the slope of the solid line in Fig.4 to be about 13.4 kcal/mole. This is in good agreement with the value of 14.7 kcal/mole obtained by Gray[3].

For temperatures below 500°C,  $A_{\text{Cs-134}}$  had an almost constant value of about  $8 \times 10^{-10}$  Ci/ $\text{cm}^3$  after four reheatings up to 1000°C, 900°C, 900°C and 700°C in this order (Fig.2). This is probably because the vapor containing Cs-134 condenses into fine particles, which easily suspend inside the canister at temperatures below 500°C.

In conclusion, the results obtained show that the amount of Cs-134 suspended in the air inside the canister ( $A_{\text{Cs-134}}$ ) has an almost

constant value of  $8 \times 10^{-10}$  Ci/cm<sup>3</sup> for temperatures of less than 500°C after several reheatings up to a maximum of 1000°C when the glass contains 0.44 Ci of Cs-134. Therefore, the amount of cesium suspended in the air inside the canister is considered to be significant even at waste storage temperatures after the glass has been subjected to several reheatings up to a maximum of 1000°C.

#### REFERENCES

1. S. TASHIRO, J. MORITA, T. TSUBOI, S. KIKKAWA, U. SHIOTA and A. TANIGUCHI, "Vitrification Apparatus (Design and Performance Test)," Report JAERI-M 84-044, Japan Atomic Energy Research Institute (March 1984).
2. H. OTSUKA, Y. TAMURA, M. NOMURA and S. TASHIRO, "Development of Gamma-Scanning System for Vitrified HLLW Forms," Report JAERI-M 84-067, Japan Atomic Energy Research Institute (April 1984).
3. W. J. GRAY, "Volatility of a Zinc Borosilicate Glass Containing Simulated High-Level Radioactive Waste," BNWL-2111, Battelle Pacific Northwest Laboratories (October 1976).



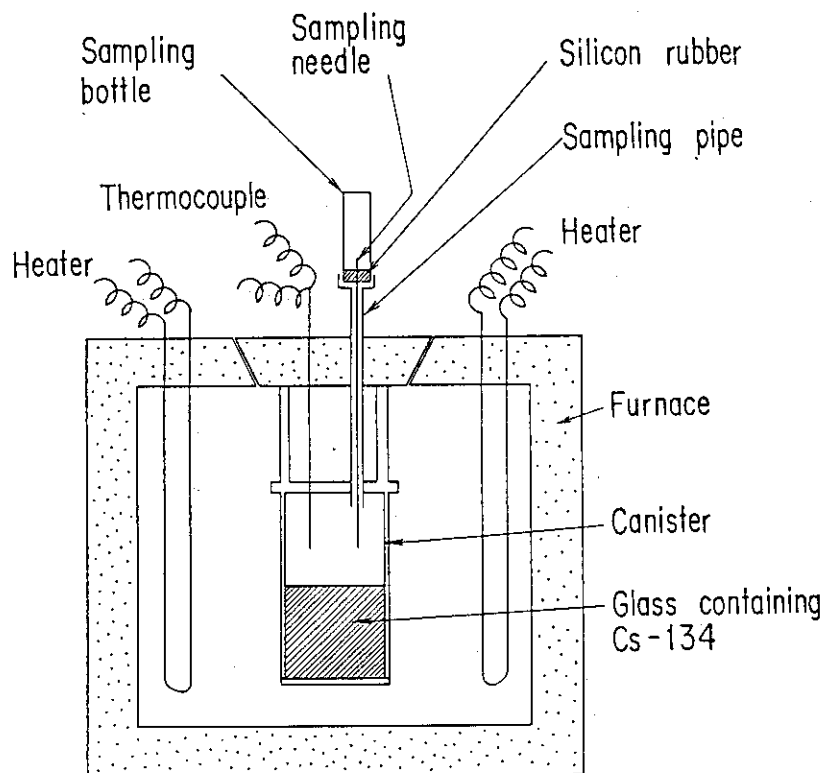


Fig.1 Schematic drawing of the apparatus.

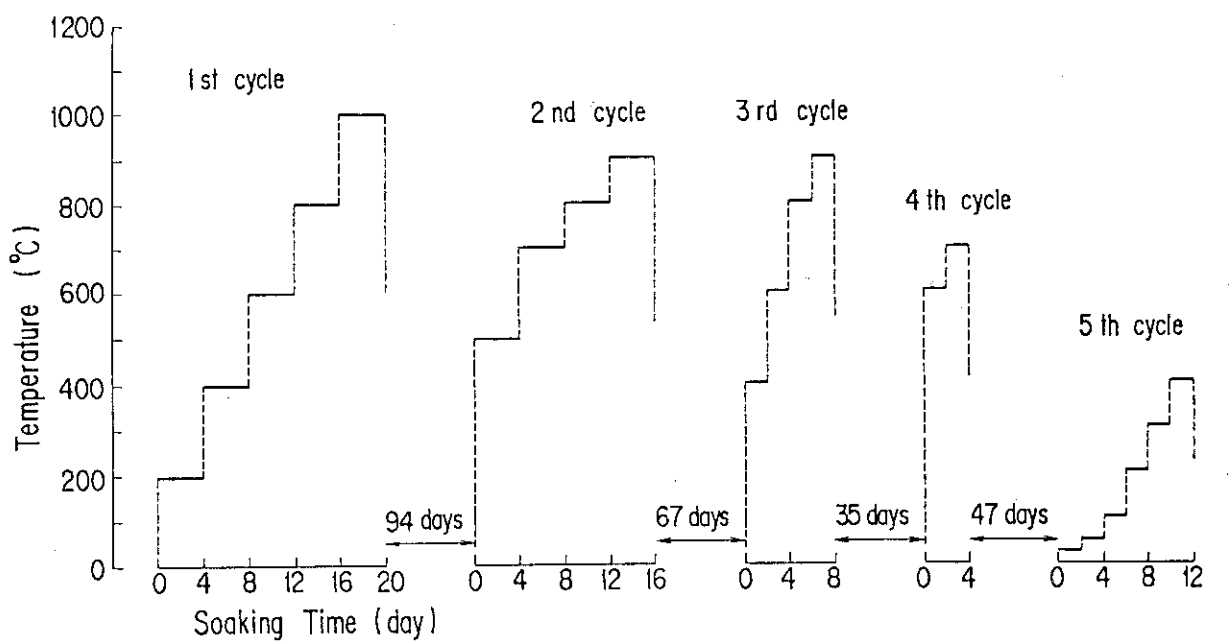


Fig.2. Schematic heating conditions. Solid lines in this figure show the position where samplings of the air inside the canister were made.

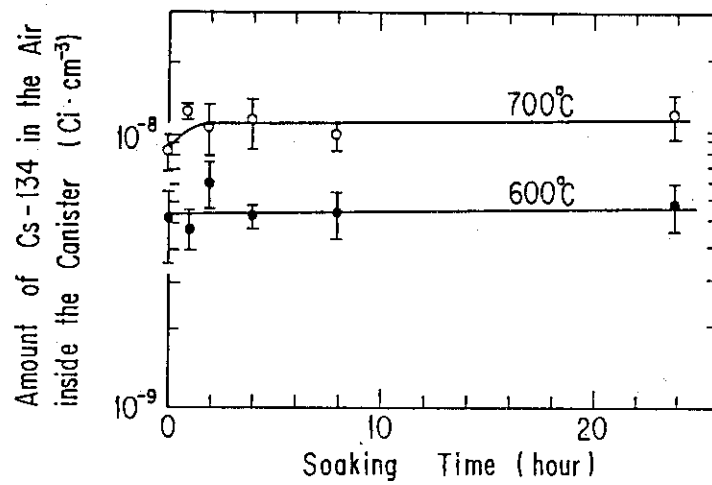


Fig.3. Time-dependency of the amount of Cs-134 suspended in the air inside the canister at 600°C and 700°C. The data were collected during the fourth cycle of reheating. The error bars show the standard deviation of each plot.

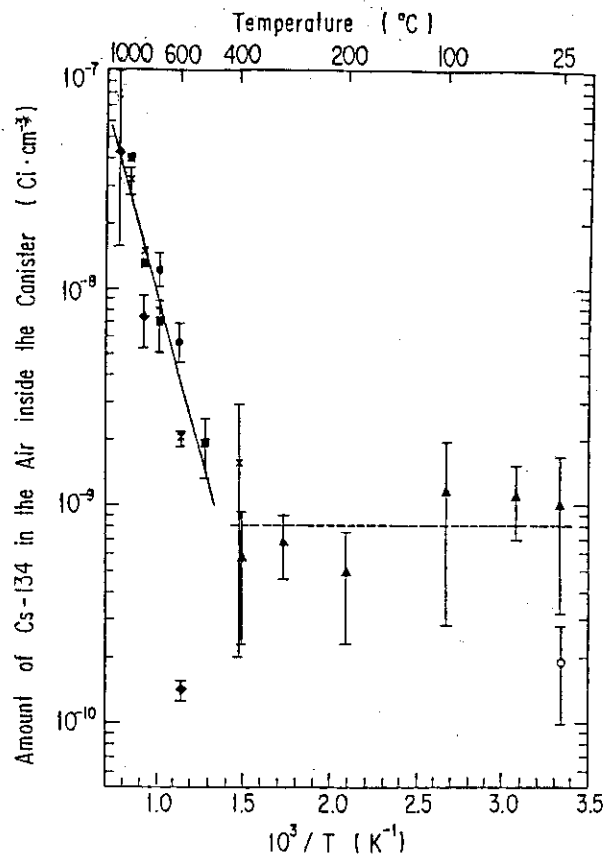


Fig.4. Temperature-dependency of the amount of Cs-134 suspended in the air inside the canister at a fixed soaking time of 1 day. The data were collected during the first cycle of reheating up to 1000°C (◆), the second cycle up to 900°C (■), the third cycle up to 900°C (×), the fourth cycle up to 700°C (●) and the fifth cycle up to 400°C (▲), which correspond to Fig.2. The error bars show the standard deviation of each plot.

### 3.5 Characterization of waste form to be returned from over-sea reprocessing

Y. Kiriyama

The  $\alpha$  radiation stability test of the HLW vitrified form to be returned has been continued. The test has been carried out by using the samples doped with short-lived  $\alpha$  nuclides (Cm-244 and Pu-238) which quantity is calculated due to TRU quantity in the real waste form. The test samples were prepared till September, 1983. After the preliminary characterization test of the sample (0 year test) was performed, the rest of samples have been stored in the capsules filling up with Ne gas in the thermostat. Up to now, 500 and 1,000 years tests were already performed after 9.7 and 13.5 months storage respectively. The tests will be continued till July of this year to obtain 10,000 years test results.

4. Safety study of nuclear facilities of vitrified HLW's stream

T. Takeda

Last year, we discussed the safety storage facilities constructed on surface, based on the safety analysis document set tentatively referred to the facilities.

The conclusion is that there are no special problems for the storage facility, because we have a lot of experiences for spent fuel storage and the waste contains few amount of fissionable elements, however, data base for evaluation of source term at accidents should be obtained experimentally more in detail.

The experiments have been carried out in WASTE-F, and the report last year is being used for governmental discussion on acceptability of characteristics of the waste to be returned.

In this year, we have proceeded to the discussions of the underground storage facilities. This is constructed and used as preceding stage of final disposal. Therefore, we have studied and discussed what the underground storage is, what a probable facility will be constructed in Japan, and what major factors are in actual safety examinations.

The safety of the preclosure of geological disposal is almost same as general nuclear facilities. Major factors in actual safety examination are items regarding on accidental cases, in which the accident of canister drop in vertical hole was considered to be the severest accident. The source terms at the accidents will be powder, which will originated from Cs deposited on inner surface and glass fractured by mechanical shock.

We will reconsider to discuss the safety assessment on accidents in the preclosure process of geological disposal as the major items in the next 5 year program.